Upgrading Root Physiology for Stress Tolerance by Ectomycorrhizas: Insights from Metabolite and Transcriptional Profiling into Reprogramming for Stress Anticipation[1][C][W][OA]

Zhi-Bin Luo, Dennis Janz, Xiangning Jiang, Cornelia Göbel, Henning Wildhagen, Yupeng Tan, Heinz Rennenberg, Ivo Feussner, and Andrea Polle*

College of Life Sciences, Northwest Agriculture & Forestry University, Yangling, Shaanxi 712100, People's Republic of China (Z.-B.L.); Büsgen Institute, Department for Forest Botany and Tree Physiology (Z.-B.L., D.J., A.P.), and Albrecht-von-Haller Institute for Plant Sciences, Department for Plant Biochemistry (C.G., I.F.), Georg-August University, 37077 Goettingen, Germany; College of Life Sciences and Biotechnology, Beijing Forestry University, Beijing 100083, People's Republic of China (X.J., Y.T.); and Institute of Forest Botany and Tree Physiology, Chair of Tree Physiology, Albert-Ludwigs University, 79110 Freiburg, Germany (H.W., H.R.)

Ectomycorrhizas (EMs) alleviate stress tolerance of host plants, but the underlying molecular mechanisms are unknown. To elucidate the basis of EM-induced physiological changes and their involvement in stress adaptation, we investigated metabolic and transcriptional profiles in EM and non-EM roots of gray poplar (*Populus* × *canescens*) in the presence and absence of osmotic stress imposed by excess salinity. Colonization with the ectomycorrhizal fungus *Paxillus involutus* increased root cell volumes, a response associated with carbohydrate accumulation. The stress-related hormones abscisic acid and salicylic acid were increased, whereas jasmonic acid and auxin were decreased in EM compared with non-EM roots. Auxin-responsive reporter plants showed that auxin decreased in the vascular system. The phytohormone changes in EMs are in contrast to those in arbuscular mycorrhizas, suggesting that EMs and arbuscular mycorrhizas recruit different signaling pathways to influence plant stress responses. Transcriptome analyses on a whole genome poplar microarray revealed activation of genes related to abiotic and biotic stress responses as well as of genes involved in vesicle trafficking and suppression of auxin-related pathways. Comparative transcriptome analysis indicated EM-related genes whose transcript abundances were independent of salt stress and a set of salt stress-related genes that were common to EM non-salt-stressed and non-EM salt-stressed plants. Salt-exposed EM roots showed stronger accumulation of myoinositol, abscisic acid, and salicylic acid and higher K^+-to-Na^+ ratio than stressed non-EM roots. In conclusion, EMs activated stress-related genes and signaling pathways, apparently leading to priming of pathways conferring abiotic stress tolerance.

Under natural conditions, many economically important tree species including fast-growing poplars (*Populus* spp.) form ectomycorrhizas (EMs) between roots and EM fungi. Colonization with EM fungi leads to profound changes in root architecture and morphology. Usually, EM roots are strongly ramnified and EM root tips show a bulb-like appearance (Smith and Read, 2008). In EMs, plants and fungi interact mutualistically: while the plant receives mineral nutrients and water through the fungus, the fungus is supplied with carbohydrates by its host (Smith and Read, 2008). To fulfill these functions, specific anatomical structures are established, which involve the formation of a hyphal mantle ensheathing the root tip with hyphae emanating into soil for nutrient uptake. Inside the mantle, hyphae grow between, but not inside, the cortex cells within the cell wall, forming an interface called the Hartig net for bidirectional nutrient exchange.

The establishment of EMs requires a coordinated developmental program in both partners of the symbiosis. Transcriptional changes during initial stages of host recognition and colonization have been the focus of several recent studies (Johansson et al., 2004; Duplessis et al., 2005; Le Queré et al., 2005; Morel et al., 2005; Wright et al., 2005; Frettinger et al., 2007; Heller

[1] This work was supported by the Deutsche Forschungsgemeinschaft (grants to A.P. and H.R. via FOR496 [Poplar Research Group, Germany]), by the Deutscher Akademischer Austauschdienst (postdoctoral scholarship to Z.-B.L. in the program Modern Application of Biotechnology), and by the Program for New Century Excellent Talents in Universities from the Ministry of Education of China (grant no. NCET–08–0468 to Z.-B.L.).

* Corresponding author; e-mail apolle@gwdg.de.

The author responsible for distribution of materials integral to the findings presented in this article in accordance with the policy described in the Instructions for Authors (www.plantphysiol.org) is: Andrea Polle (apolle@gwdg.de).

[C] Some figures in this article are displayed in color online but in black and white in the print edition.

[W] The online version of this article contains Web-only data.

[OA] Open Access articles can be viewed online without a subscription.

www.plantphysiol.org/cgi/doi/10.1104/pp.109.143735

et al., 2008). Furthermore, the molecular and physiological alterations required to maintain steady-state functions of EMs with respect to nutrient exchange, in particular regarding carbon and nitrogen, have been studied (Martin et al., 2007; Nehls, 2008).

In addition to improving plant nutrition, EMs also increase plant protection from soil-borne stresses (Schützendübel and Polle, 2002; Polle and Schützendübel, 2003). Mycorrhizal plants exposed to osmotic constraints generally perform better than nonmycorrhizal plants (Shi et al., 2002; Bogeat-Triboulot et al., 2004; Bois et al., 2006; Valdes et al., 2006; Langenfeld-Heyser et al., 2007). On the global scale, osmotic stresses caused by soil salinization and water limitations are the most important factors reducing plant production (Food and Agriculture Organization of the United Nations, Land and Plant Nutrition Management Service; http://www.fao.org/ag/agl/agll/spush). High soil salinity limits water uptake and results in metabolic disorders, ion imbalances, and oxidative stress when excess sodium is accumulated (Munns and Tester, 2008). Recently, EM-forming fungi such as the basidiomycete *Paxillus involutus* have been identified that are highly salt tolerant and can attenuate detrimental salt effects in their host plants (Langenfeld-Heyser et al., 2007). Suitable EM fungi, therefore, have a high potential to increase plant biomass production on salt-affected soils.

In spite of the importance of EM associations for plant vitality, we have little information on the molecular and physiological mechanisms underlying improved stress protection. Most of our knowledge comes from crop plants that interact with arbuscular mycorrhizas (AMs), which differ in many respects from EM fungi. AM fungi are obligate biotrophs, since they cannot grow in the absence of their host, whereas EM fungi also proliferate saprotrophically as free-living organisms (Martin et al., 2008). AM fungi invade root cells with hyphal growth from cell to cell and form extended arbuscule-like structures and vesicles within the cells. It has been suggested that AMs trigger mycorrhiza-induced resistance (MIR), which improves stress tolerance of mycorrhizal compared with nonmycorrhizal plants (Pozo and Azcon-Aguilar, 2007). Unlike systemic acquired resistance, which involves salicylic acid (SA; Vlot et al., 2008), MIR is thought to induce SA only during the initial stage of infection (Pozo and Azcon-Aguilar, 2007). Subsequently, SA accumulation is suppressed and jasmonic acid (JA)-related pathways are recruited (Pozo and Azcon-Aguilar, 2007). However, there are contrasting reports on JA and SA levels and functions in plants associated with AM fungi (Barker and Tagu, 2000; Ludwig-Müller, 2000; Hause et al., 2007; Riedel et al., 2008). Furthermore, auxin (indole acetic acid [IAA]) and abscisic acid (ABA) have been invoked in AM formation (Barker and Tagu, 2000; Herrera-Medina et al., 2007; Pozo and Azcon-Aguilar, 2007). While both of these phytohormones are important for the orchestration of developmental processes, ABA is also involved in signaling and defense processes against drought or salinity (Yamaguchi-Shinozaki and Shinozaki, 2006). After long-term colonization by AM fungi, increases in the expression of genes involved in signaling and defense processes have been observed in the host (Liu et al., 2007). However, the links between mycorrhiza-induced activation of stress-related genes and improved plant stress tolerance have not yet been investigated.

In this study, we used gray poplar (*Populus* × *canescens* = *Populus tremula* × *Populus alba*), which has high productivity and high salt sensitivity (Bolu and Polle, 2004; Ehlting et al., 2007), to characterize anatomical, physiological, and molecular adaptations of roots as a consequence of colonization with *P. involutus*. Nutrient status, carbohydrates, and endogenous phytohormone levels were measured in EM compared with non-EM roots. We conducted genome-wide transcriptional analysis to identify long-term EM-responsive root genes using whole genome poplar microarrays. Since we found EM-induced activation of abiotic and biotic defense pathways as well as carbohydrate accumulation and increases in ABA and SA, we hypothesized that enhanced host resistance is related to priming for osmotic stress. To test this hypothesis, mycorrhizal and nonmycorrhizal poplars were exposed to high salinity and used for comparative metabolite and transcriptome analysis. By this strategy, (1) stress-independent EM-associated and (2) overlapping stress-specific gene clusters were identified in the EM-responsive transcriptome of poplar roots.

RESULTS

EMs Reshape the Morphology and Physiology of Root Cells

Poplar roots inoculated with the fungus *P. involutus* developed typical EM structures, such as the hyphal mantle and the Hartig net (Fig. 1, A and D). EM colonization was found on 63% ± 2% of the root tips. Noninoculated plants did not show any mycorrhizas. EM colonization changed root architecture, because the roots contained relatively more fine roots than non-EM roots (Table I). Peripheral root cells of EM plants were swollen in comparison with non-EM root cells, resulting in about 3- to 4-fold higher cross-sectional area per cell (Table I).

Volume changes of cells require increased water uptake, which is achieved by accumulation of osmotically active compounds (Polle et al., 2006). To investigate whether the profound cellular changes observed under the influence of EMs were associated with accumulation of osmolytes, we determined soluble carbohydrates, sugar alcohols, free amino acids including ammonium, and the concentrations of mineral nutrient elements (Fig. 2; Table II). EMs caused increases in total soluble carbohydrate concentrations.

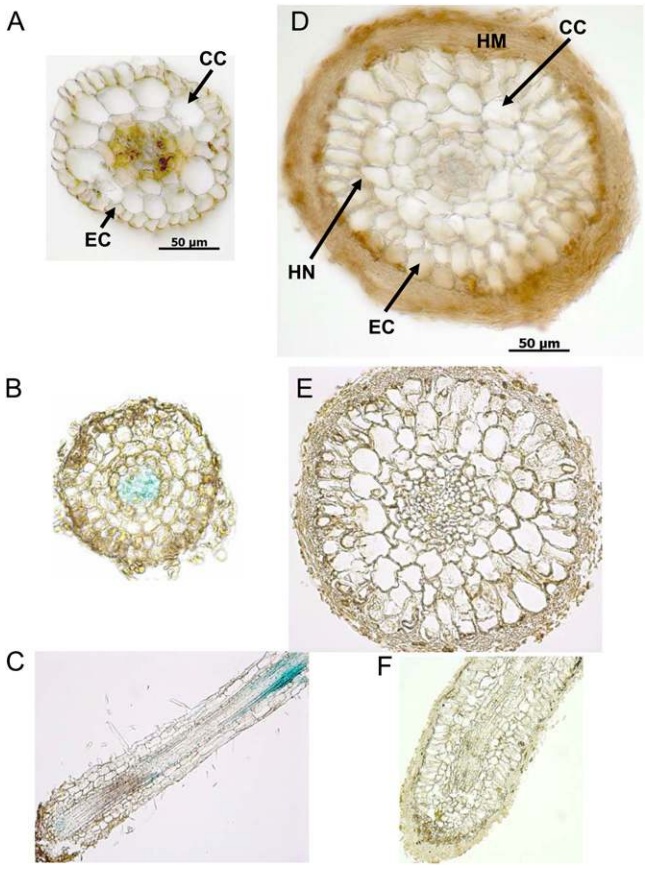

Figure 1. Anatomical characteristics of nonmycorrhizal (A) and ectomycorrhizal (D) root tips of wild-type poplar (*P.* × *canescens*) and of poplar line 51 transformed with the auxin-responsive GH3::GUS reporter (cross sections [B and E] and longitudinal sections [C and F]) of nonmycorrhizal (B and C) and mycorrhizal (E and F) root tips. EC, Epidermal cell; CC, cortical cell; HM, hyphal mantle; HN, Hartig net. Representative micrographs are shown. Blue staining indicates GUS activity. Line 31 yielded the same staining pattern. [See online article for color version of this figure.]

The most abundant carbohydrate was Suc (Fig. 2A), a compound that cannot be metabolized by EM (Nehls, 2008). Carbohydrates with chaperone-like activity, such as myoinositol, sorbitol, and mannitol, were also significantly increased in EMs [for mycorrhizal versus nonmycorrhizal plants, $P_{(\text{myoinositol})} = 0.003$, $P_{(\text{sorbitol})} < 0.001$, $P_{(\text{mannitol})} < 0.001$; Fig. 2, A and B]. Trehalose was 9-fold higher in EM than in non-EM roots ($P < 0.001$; Fig. 2B). Among free amino acids, Gln and Asn were significantly increased in EM roots ($P < 0.001$; Fig. 2C). Many amino acids were below the detection limit under all experimental conditions (Ile, Lys, Met, Orn, Gly, Cys, Val, Tyr, and Phe). Cation concentrations were unaffected in EM compared with non-EM roots (Fig. 2D). Among other nutrient elements, a trend toward increased nitrogen and significantly increased phosphorus concentrations was found in EM compared with non-EM roots (Table II).

As sugar alcohols usually accumulate under osmotic stress, we suspected that stress pathways might have been activated in EM roots. Indeed, EM roots contained increased concentrations of the stress signaling compounds SA and ABA, whereas JA as well as JA-Ile, its active amino acid conjugate, and precursor, 12-oxo-phytodienoic acid (oPDA), were decreased (Table III). In the absence of stress, auxin was decreased in EM compared with non-EM root tips ($P \leq 0.05$; Table III). This observation was corroborated by analysis of GH3::GUS reporter plants, which showed activation of the auxin-responsive GH3 promoter in developing vascular structures only in non-EM and not in EM root tips (Fig. 1, B, C, E, and F).

Since hormonal compounds of fungal origin may influence root physiology, we also measured phytohormone levels in saprophytically grown *P. involutus* mycelia. However, SA, JA, JA-Ile, and ABA were not detected. The mycelia contained low amounts of IAA similar to those present in mycorrhizal roots (0.102 ± 0.79 nmol g^{-1} dry weight).

Transcriptional Profiling Reveals Major Effects of EMs on Stress Response and Signaling Pathways

To investigate the molecular basis of altered physiology and morphology of EM roots, we conducted genome-wide transcriptional profiling using poplar microarrays. Out of 61,251 probe sets represented on the array, the transcriptional responses of only 168 genes (i.e. 0.3%) were changed in EM roots (Supplemental Table S1). Quantitative reverse transcription (qRT)-PCR showed the reliability of the method (Supplemental Fig. S1). Among the *P. involutus*-responsive genes (PiRGs), 92 showed increased and 76 showed decreased transcript levels, of which 33 had no match in Arabidopsis (*Arabidopsis thaliana*; Supplemental Table S1). For the remaining PiRGs, Arabidopsis Genome Initiative (AGI) annotations were obtained. Since several PiRGs gave matches with the same Arabidopsis gene, a total of 67 and 58 unique genes with increased and decreased transcript levels, respectively, could be assigned to AGI numbers (Supplemental Tables S2 and S3).

MapMan was used to assign genes with AGI numbers to functional groups (Thimm et al., 2004; Usadel et al., 2005). Among 125 genes with AGI numbers, significantly higher numbers were present in the MapMan categories Stress ($P = 0.009$), Signaling ($P = 0.033$), and Miscellaneous ($P = 0.034$ for cytochrome P450 and $P = 0.034$ for acid and other phosphatases). Forty-two genes (33% of all PiRGs) were retrieved in the MapMan pathway Biotic Stress (Supplemental Fig. S2).

Signal Transduction and Stress Response

The category Stress contained six increased PiRGs (Bet v I allergen family protein, DNA J heat shock protein, two germin-like proteins [GLP subfamily T

Table I. *Size of peripheral root cells, fine-to-coarse root ratio, and dry mass of mycorrhizal (M) or nonmycorrhizal (N) P. × canescens under control conditions (C) or after exposure to salt stress (S)*

Data indicate means ± SE ($n = 30$ for cell counts and $n = 16$ for root ratio and dry mass). Calculated P values are indicated for the effects of mycorrhiza $P_{(EM)}$ and salt stress $P_{(salt)}$.

Treatment	Cell Area	Fine-to-Coarse Root Ratio	Belowground Biomass	Aboveground Biomass
	μm^2		g	g
NC	169.3 ± 13.8	0.56 ± 0.05	3.77 ± 0.22	2.38 ± 0.24
NS	139.8 ± 10.0	0.35 ± 0.04	3.64 ± 0.49	2.61 ± 0.24
MC	640.2 ± 42.5	0.73 ± 0.03	3.94 ± 0.64	2.79 ± 0.37
MS	474.7 ± 30.1	0.56 ± 0.06	3.81 ± 0.59	2.48 ± 0.31
$P_{(EM)}$	0.0000	0.0015	0.7372	0.6462
$P_{(salt)}$	0.0006	0.0013	0.7825	0.8698

and GLP2a], Ser protease inhibitor, and trypsin protease inhibitor; Fig. 3) and only one decreased PiRG (DDB2 [for damaged DNA-binding 2]; Fig. 3). The category Signaling contained three PiRGs with increased (general regulatory factor 9, photoassimilate-responsive protein, and transducin family protein; Fig. 3) and six with decreased (MAP [for mitogen-activated protein] kinase 19, MAP kinase 9 protein kinase-like, COP1-interacting protein-like, inositol-1,3,5-trisphosphate 5/6 kinase family protein, Leu-rich repeat protein, and rho-GTPase-activating-like protein; Fig. 3) transcript levels.

The category RNA Regulation contained stress-associated transcription factors with increased levels: BPC4/BBR, bHLH family protein, DNA-binding protein, myc family, TCP family, WRKY2, WRKY40, and RD26 (Fig. 3). RD26 (for responsive to desiccation 26) is a transcriptional activator in ABA-mediated dehydration response (Yamaguchi-Shinozaki et al., 1992). Most of the transcription factors with diminished levels (AS1, CLF, HAP2a, DDB2, HB-17, MYB36, BRM/CHR2, and Pro-rich family protein; Fig. 3) are involved in developmental processes, and AS1 is known to be regulated by auxin (Yang et al., 2008).

Metabolism and Cell Functions

PiRGs in the category Protein Metabolism showed some overlap with Stress and RNA Regulation and furthermore contained a chaperonin-like protein with increased components of the proteasome complex (cullin 1, zinc finger protein-like) and decreased transcript levels (Fig. 3). Cullin 1 may be involved in mediating auxin and jasmonate responses (Woodward et al., 2007).

Secondary Metabolism

The category Secondary Metabolism contained decreased transcript levels of a putative cytochrome reductase (CYP450 reductase), an enzyme that transfers electrons to P450s. The closest Arabidopsis ortho-

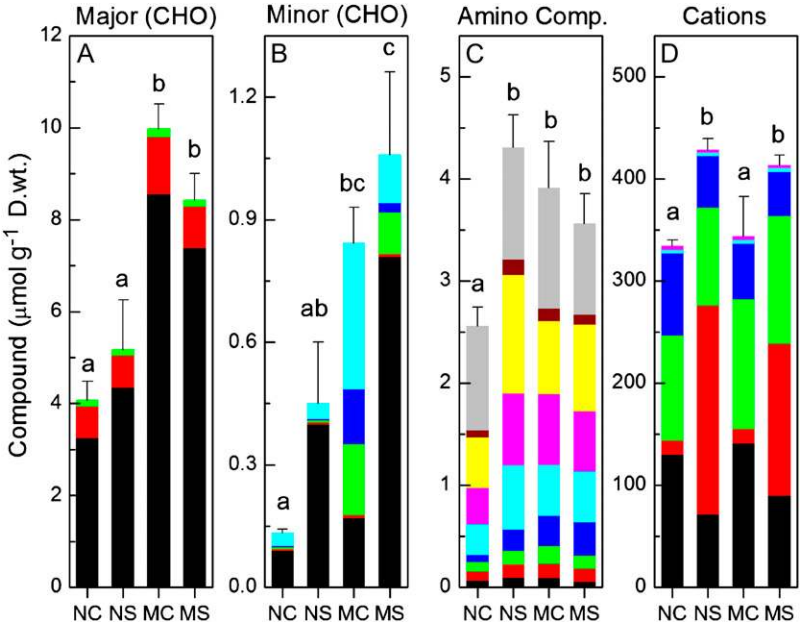

Figure 2. Soluble carbohydrates (CHO) of major pathways (A; Suc, black; Glc, red; Fru, green) and minor pathways (B; myoinositol, black; Gal, red; mannitol, green; sorbitol, blue; trehalose, cyan), amino compounds (C; Pro, black; Ser, red; Ala, green; Asn, blue; Asp, cyan; Gln, pink; Glu, yellow; γ-aminobutyric acid, burgundy; NH_4^+, gray), and cations (D; potassium, black; sodium, red; calcium, green; magnesium, blue; iron, cyan; manganese, pink) in mycorrhizal (M) or nonmycorrhizal (N) fine roots of *P. × canescens* under control conditions (C) or after exposure to salt stress (S). Data indicate means ± SE ($n = 4$). Different letters indicate significant difference for the sum of each metabolite class between the treatments at $P \leq 0.05$. D.wt., Dry weight.

Table II. *Concentrations (mg g^{-1} dry weight) of major nutrient elements in fine roots of mycorrhizal (M) or nonmycorrhizal (N) P. × canescens under control conditions (C) or after exposure to salt stress (S)*

Data indicate means ± SE ($n = 4$). Calculated P values are indicated for the effects of mycorrhiza $P_{(EM)}$ and salt stress $P_{(salt)}$.

Treatment	Carbon	Nitrogen	Phosphorus	Sulfur
NC	470 ± 5	6.8 ± 0.5	0.52 ± 0.01	1.46 ± 0.06
NS	467 ± 2	6.1 ± 0.3	0.54 ± 0.01	1.20 ± 0.05
MC	469 ± 2	7.6 ± 0.4	1.16 ± 0.15	1.35 ± 0.19
MS	454 ± 1	6.6 ± 0.4	1.29 ± 0.04	1.38 ± 0.06
$P_{(EM)}$	0.3134	0.1116	0.0000	0.7912
$P_{(salt)}$	0.2277	0.0575	0.3700	0.3031

log to the poplar CYP450 reductase AR1 has been invoked in phenylpropanoid metabolism (Mizutani and Ohta, 1998). This prompted us to compare phenolic compounds in non-EM and EM roots (Fig. 4). Visualization of phenolic compounds in root cross sections suggested stronger incorporation of phenolics in the vascular system of non-EM compared with EM roots and suppression of phenolic incorporation in cell walls of root cells harboring the Hartig net (Fig. 4).

Lipid Metabolism

PiRGs in the category Lipid Metabolism pointed to suppression of brassinolide biosynthesis, increased turnover of lipids, and activation of desaturases. However, the composition of fatty acids was not changed (Supplemental Table S4), which confirms earlier findings (Reich et al., 2009).

Phospholipase 2 (PLP2), which has wide substrate specificity and accumulates upon infection by fungal and bacterial pathogens (La Camera et al., 2005, 2009), had increased transcript levels (Fig. 3). This was also true for clathrin coat assembly protein (Cell Function), which is involved in vesicle transport to the plasma membrane (Edeling et al., 2006), and for Yip1 (category Not Assigned; Fig. 3), an integral membrane protein required for the biogenesis of endoplasmic reticulum-derived COPII transport vesicles (Heidtman et al., 2005). Activation of secretory processes may be required for the formation of enlarged root cells. In contrast, phospholipase PLPζ2, which is involved in vesicle trafficking responsible for auxin distribution (Li and Xue, 2007), was suppressed.

Metabolite Transport

Only a few transport proteins were affected at the transcriptional level. Increases were found for proton-dependent oligopeptide transport family protein 14 and a high-affinity ammonium transporter of subfamily 2 (Fig. 3); decreases were observed for a glycerol-3-phosphate transporter and a heavy metal-associated domain-containing protein (Fig. 3). Database searches showed that *Paxillus*-responsive ammonium transporter had been annotated as AMT3;1 (Couturier et al., 2007). To confirm that *AMT3;1* was expressed in fine roots of *P.* × *canescens*, RT-PCR was carried out using gene-specific primers and the PCR product was sequenced. The sequence data confirmed 96.6% and 95.5% identity for *AMT3;1* at the cDNA and amino acid levels between *P.* × *canescens* and *P. trichocarpa*, respectively (Supplemental Fig. S3). To further confirm that *AMT3.1* was induced in fine roots by *P. involutus*, qRT-PCR was performed using gene-specific primers, and the results of qRT-PCR were in agreement with the array data (Supplemental Fig. S1).

Cell Wall

Furthermore, we found evidence for changes in cell wall composition, since transcripts for pectin methylesterase and Pro-rich protein decreased and those for expansin A6 and cellulose synthase-like B4 increased (Fig. 3).

Other Categories

In the categories Minor Carbohydrate Metabolism (galactinol synthetase), Glycolysis (glyceraldehyde-3-phosphate dehydrogenase), N Metabolism (Glu dehydrogenase), Redox (a cytochrome b561-1 [ACYB-1]), and Miscellaneous, four cytochrome P450 oxidases showed increased transcript levels in response to EM colonization, whereas Amino Acid Metabolism with acetoacetyl-CoA thiolase 2 and Asp-Glu racemase and Co-factor and Vitamin with riboflavin biosynthesis

Table III. *Concentrations of phytohormones (nmol g^{-1} dry weight) in fine roots of mycorrhizal (M) or nonmycorrhizal (N) P. × canescens under control conditions (C) or after exposure to salt stress (S)*

Data indicate means ± SE ($n = 4$). Calculated P values are indicated for the effects of mycorrhiza $P_{(EM)}$ and salt stress $P_{(salt)}$. Different letters in columns indicate significant differences at $P \leq 0.05$.

Treatment	SA	ABA	IAA	JA	JA-Ile	oPDA
NC	0.479 ± 0.009 a	0.013 ± 0.007 a	0.355 ± 0.008 b	0.230 ± 0.007 b	0.225 ± 0.008 d	18.750 ± 0.008 c
NS	1.318 ± 0.009 b	0.080 ± 0.007 b	0.084 ± 0.009 a	0.081 ± 0.005 a	0.038 ± 0.007a	5.212 ± 0.006 a
MC	0.661 ± 0.007 a,b	0.025 ± 0.008 a	0.126 ± 0.007 a	0.121 ± 0.006 a	0.114 ± 0.005 c	10.471 ± 0.006 b
MS	3.802 ± 0.008 c	0.127 ± 0.008 b	0.127 ± 0.009 a	0.120 ± 0.007 a	0.060 ± 0.006 b	8.279 ± 0.008 a,b
$P_{(EM)}$	0.0195	0.0249	0.2446	0.0032	0.4298	0.0144
$P_{(salt)}$	0.0002	0.0000	0.0162	0.0005	0.0000	0.0001

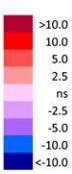

Putative function	AGI	PiRG	EMAG	STAG	MSAG	Putative function	AGI	PiRG	EMAG	STAG	MSAG
minor CHO											
ATGOLS2 (Arabidopsis thaliana galactinol synthase 2)	At1g56600	2.03	ns	3.4	ns						
Glycolysis											
GAPC (Glyceraldehyde3-phosphate dehydrogenase ubunit)	At3g04120	1.94	ns	4.5	2.46						
GAPC-2; glyceraldehyde-3-phosphate dehydrogenase	At1g13440	10.79	4.9	ns	ns						
Fermentation											
ALDH7B4 (Aldehyde dehydrogenase 7B4)	At1g54100	2.36	ns	ns	ns	ALDH2B4 (aldehyde dehydrogenase 2)	At3g48000	-2.33	ns	-2.3	ns
Cell wall											
ATCSLB04 (Cellulose synthase-like B4);	At2g32540	3.56	2.8	ns	ns	ATPME3 (Arabidopsis thaliana pectin methylesterase 3)	At3g14310	-2.56	ns	-2.1	-3.73
ATEXPA6 (Arabidopsis thaliana expansin-A6)	At2g28950	1.77	ns	ns	ns	PRP4 (proline-rich Protein 4)	At4g38770	-6.67	ns	ns	ns
Lipid metabolism											
SLD1 (delta-8 sphingolipid desaturase, putative)	At2g46210	7.77	6.5	ns	ns	PLDP2 (phospholipase D ZETA 2)	At3g05630	-4.35	-2.8	ns	ns
FATB (acyl carrier/acyl-ACP thioesterase B)	At1g08510	8.97	3.1	ns	ns	SQD2 (Sulfoquinovosyldiacylglycerol transferase 2)	At5g01220	-2.38	ns	ns	ns
FQR1 (flavodoxin-like quinone reductase 1)	At5g54500	2.39	ns	ns	-3.6	squalene monooxygenase, putative	At2g22830	-4.17	ns	ns	ns
						SRG3 (Senescence realted gene 3)	At3g02040	-3.23	ns	ns	ns
N metabolism and amino acid metabolism											
GDH 3 (glutamate dehydrogenase 3, putative)	At3g03910	1.87	ns	ns	ns	ACAT2/EMB1276 (acetoacetyl-CoA thiolase 2)	At5g48230	-2.08	ns	ns	ns
						aspartate-glutamate racemase family	At1g15410	-6.25	ns	ns	ns
Secondary metabolism											
FAD-binding domain-containing protein	At1g30700	2.66	ns	6.9	4.22	ACAT2/EMB1276 (acetoacetyl-CoA thiolase 2)	At5g48230	-2.08	ns	ns	ns
OMT2 (O-methyltransferase family 2 protein)	At4g35160	1.85	ns	ns	ns	ATR1 (Arabidopsis cytochrome reductase, cyp450)	At4g24520	-2.17	ns	ns	ns
2OG-Fe(II) oxygenase family protein	At4g10490	4.13	ns	ns	ns						
UGT72B1 (UDP-glucosyl transferase family protein	At4g01070	2.56	1.9	ns	2.54						
Hormone metabolism											
GASA5 (gibberellin-regulated family protein, putative)	At3g02885	1.83	ns	2.4	ns	squalene monooxygenase, putative	At2g22830	-4.17	ns	ns	ns
Co-factor and vitamine metabolism											
						riboflavin biosynthesis protein,	At2g22450	-8.33	ns	ns	ns
Stress											
Bet v I allergen family protein, identical to MLP-like protein 423	At1g24020	18.12	8.9	ns	ns	DDB2 (damaged DNA binding 2), transducin family protein	At5g58760	-1.61	ns	ns	ns
DNAJ heat shock protein, putative	At2g17880	7.80	ns	7.4	ns						
germin-like protein, putative subfamily T member 2 precursor	At1g18980	5.46	ns	ns	ns						
GLP2A (Germin-like protein 2A)	At5g39190	3.55	ns	25	8.03						
serine protease inhibitor, Kazal-type family protein	At3g61980	1.56	ns	3.8	ns						
trypsin and protease inhibitor family protein / Kunitz family protein	At1g73260	6.82	ns	45	7.73						
Redox											
ACYB-1 (Arabidopsis cytochrome b561 -1)	At5g38630	1.62	ns	ns	ns						
Miscellaneous											
ATGSTU4 (glutathione transferase 22), tau class	At2g29460	1.84	ns	3.6	2.21	ATACP5 (acid phosphatase 5)	At3g17790	-7.69	-4.3	ns	ns
CYP71B34 (cyt P450, family 71, subfamily B, polypeptide 34)	At3g26300	5.59	4.1	ns	ns	ATPAP3/PAP3 (purple acid phosphatase 3)	At1g14700	-1.92	ns	ns	ns
CYP78A5 (cyt P450, family 78, subfamily A, polypeptide5)	At1g13710	3.31	ns	ns	ns	ATR1 (Arabidopsis cytochrome reductase, cyp450)	At4g24520	-2.17	ns	ns	ns
CYP78A7 (cyt P450, family 78, subfamily A, polypeptide 7)	At5g09970	8.76	3.6	ns	-3.57	calcineurin-like phosphoesterase family,similar to ATPAP24	At1g13750	-2.94	ns	ns	ns
CYP81K2 (cyt P450, family 81, subfamily K, polypeptide 2)	At5g10600	4.35	2.3	ns	ns	PAP10; protein serine/threonine phosphatase	At2g16430	-2.94	-1.9	ns	ns
FAD-binding domain-containing protein	At1g30700	2.66	ns	ns	4.22	protein arginine N-methyltransferase family protein	At3g20020	-1.79	ns	ns	ns
LTP (protease inhibitor/seed storage/lipid transfer protein)	At3g18280	1.71	ns	-2.8	-4.48	SDR (short-chain dehydrogenase/reductase family)	At4g24050	-2.33	ns	ns	ns
UDP-glucoronosyl/UDP-glucosyl transferase family protein	At1g22340	24.03	15.3	ns	ns						
RNA regulation of transcription											
ATBPC4/BBR/BPC4/BPC4 (basic pentacysteine 4)	At2g21240	1.60	ns	ns	ns	AS1 (asymetric leaves 1); MYB-domain protein	At2g37630	-11.1	-8.4	ns	ns
bHLH (basic helix-loop-helix family protein bHLH096)	At1g22490	1.91	ns	ns	ns	ATBRM/CHR2 (Arabidopdid thaliana BRAHMA)	At2g46020	-2.13	ns	ns	ns
DNA-binding protein, similar topPentatricopeptide repeat	At1g80270	2.35	ns	ns	ns	CLF (Curly leaf)	At2g23380	-2.22	ns	ns	ns
myb family transcription factor	At1g75250	1.60	ns	ns	-3.2	DDB2 (Damaged DNA-Binding 2);transducin family protein	At5g58760	-1.61	ns	ns	ns
RD26 (responsive to dessication 26); NAC transcription factor	At4g27410	4.08	ns	ns	ns	HAP2A (Embryo defective 2220); binds to CCAAT box motif	At5g12840	-2.50	-2.2	ns	ns
TCP family transcription factor	At4g18390	1.57	ns	ns	ns	HB-17 (homeobox-leucine zipper protein 17)	At2g01430	-2.00	ns	ns	ns
WRKY2 (WRKY DNA-binding protein 2)	At5g56270	2.55	ns	ns	ns	MYB36 (myb domain protein 36)	At5g57620	-4.35	ns	ns	ns
WRKY40 (WRKY DNA-binding protein 40)	At1g80840	4.26	ns	4.0	2.2	proline-rich family protein	At5g14540	-1.96	ns	ns	ns
Protein metabolism											
RPL27aC (60S ribosomal protein L27A)	At1g70600	1.60	ns	ns	ns	ATCLPC (Caseinolytic protease C)	At3g48870	-2.04	ns	ns	ns
AtTLP3 (TUBBY like protein 3)	At2g47900	2.06	1.9	2.7	ns	ATCUL1 (Cullin 1)	At4g02570	-2.00	ns	ns	ns
chaperonin, putative	At3g02530	1.64	ns	ns	ns	ATTOC132/TOC132 (Multimericc translocon complex 132)	At2g16640	-3.23	ns	ns	ns
serine protease inhibitor, Kazal-type family protein	At3g61980	1.56	ns	ns	ns	NTF 2 (nuclear transport factor 2 family protein)	At5g43960	-1.64	ns	ns	ns
UBC10 (ubiquitin-conjugating enzyme 10)	At5g53300	1.54	ns	ns	ns	RPL2 (mitochondral 60S ribosomal protein L2, putative)	At2g07715	-2.27	ns	ns	ns
						zinc finger (C3HC4-type RING finger)	At1g17970	-4.00	ns	ns	ns
Signaling											
GRF9 (General regulatory factor 9)	At2g42590	1.67	ns	1.5	ns	ATMPK19 (Arabidopsis thaliana MAP kinase 19)	At3g14720	-9.1	ns	ns	ns
photoassimilate-responsive protein	At5g52390	3.67	ns	3.9	ns	COP1-interacting protein-related	At1g17360	-3.57	ns	ns	ns
transducin family protein (WD-40), protein kinase C receptor	At3g49180	1.68	ns	ns	ns	ITPK2 (inositol1,3,4-trisphosphate 5/6-kinase family protein 2)	At4g08170	-2.94	-1.9	ns	ns
						leucine-rich repeat family protein	At1g29740	-4.55	ns	ns	ns
						MPK9 (MAP kinase 9)	At3g18040	-1.89	ns	-1.7	ns
						protein kinase family protein	At4g39110	-3.45	ns	ns	ns
						Rho-GTPase-activating protein-related	At4g35750	-5.00	-3.3	-2.2	ns
Cell Function											
clathrin coat assembly protein, putative similar to AP19	At1g47830	1.76	ns	ns	ns	AML4 (Arabidopsis MEI2-LIKE)	At5g07290	-1.89	ns	ns	ns
						CIP7 (COP1-interacting protein 7)	At4g27430	-1.79	ns	ns	ns
Development											
PLP2 (phospholipase 2A)	At2g26560	1.62	ns	3.1	4.6	COP1-interacting protein-related	At1g17360	-3.57	ns	ns	ns
RD26 (responsive to dessication 26); NAC transcription factor	At4g27410	4.08	ns	3.9	ns						
Transport											
ATAMT2 (ammonium transporter 2)	At2g38290	3.90	8.3	-6.7	ns	glycerol-3-phosphate transporter	At3g47420	-5.56	-3.6	ns	ns
PDR14 pleiotropic drug resistance protein 14 (ABC transporter)	At4g15233	8.41	4.4	ns	ns	heavy-metal-associated domain-containing protein	At5g03380	-4.76	ns	ns	ns
POT (proton-dependent oligopeptide transport)	At1g69870	3.86	ns	ns	ns						
Not assigned											
EMB3006 (Embryo defective 3006)	At4g19350	1.63	ns	ns	ns	alanine racemase family protein	At1g11930	-5.56	ns	ns	ns
EMB3009 (Embryo defective 3009)	At5g23940	8.06	ns	ns	ns	ARG1 (Altered response to gravity 1)	At1g68370	-1.59	ns	ns	ns
EDGP (extracellular dermal glycoprotein, putative)	At1g03220	1.81	ns	4.1	3.16	similar to pentatricopeptide (PPR) repeat-containing protein	At1g62930	-3.23	ns	ns	ns
hydrolase, similar to epoxide hydrolase	At5g53050	1.81	ns	ns	ns	C2 domain-containing protein	At1g44120	-1.75	ns	ns	ns
integral membrane Yip1 family protein	At2g36300	1.54	ns	ns	ns	integral membrane family protein	At1g78620	-4.76	ns	ns	ns
oxidoreductase family protein	At4g09670	1.83	ns	ns	ns	pentatricopeptide (PPR) repeat-containing protein	At4g37380	-3.85	ns	ns	ns
RCD1 (radical-induced cell death 1)	At1g32230	1.93	ns	ns	ns	PMP 36 (peroxisomal membrane protein 36)	At2g39970	-6.25	ns	ns	ns
NTF2 (similar to nuclear transport factor 2)	At4g28910	1.60	ns	ns	ns	phosphotransferase-related similar to unknown protein	At5g43745	-1.75	ns	ns	ns
similar to unknown protein	At5g59080	18.18	ns	ns	ns	similar to AMP-dependent synthetase and ligase	At1g57680	-3.03	ns	-2.8	ns
similar to unknown protein	At3g55570	7.26	ns	ns	ns	similar to Rho-GTPase-activating protein-related	At3g10210	-2.50	-1.8	1.9	2.78
similar to unknown protein	At5g13220	4.01	ns	ns	ns	similar to unknown protein	At1g76070	-4.55	ns	ns	-1.87
similar to unknown protein	At5g02020	2.57	ns	3.5	3.57	similar to unknown protein	At1g77500	-1.82	ns	-1.6	ns
similar to unknown protein	At2g28580	2.19	ns	4.4	2.31	similar to unknown protein	At4g35920	-1.96	ns	ns	ns
similar to unknown protein	At1g68490	2.13	ns	ns	ns	similar to unknown protein	At3g59870	-5.56	ns	ns	ns
similar to unknown protein	At4g10970	1.77	ns	ns	ns	TPR3 (Topless-related 3)	At5g27030	-1.72	ns	ns	ns
similar to unknown protein	At1g55340	1.72	ns	ns	ns	Ulp1 protease family protein	At1g09730	-3.57	ns	1.5	ns
similar to unknown protein	At1g23710	4.10	2.1	ns	ns						
SPX (SYG1/Pho81/XPR1) domain-containing protein	At5g20150	2.10	-5.2	ns	ns						

Figure 3. Genes with significantly increased (red) or decreased (blue) transcript levels in mycorrhizal compared with nonmycorrhizal fine roots of *P.* × *canescens*. AGI annotations and putative functions were assigned to poplar gene models and grouped according to MapMan categories. The scale indicates increasing (R-fold) or decreasing (−1/R-fold) response factors for mycorrhizal compared with nonmycorrhizal roots without salt stress (MC/NC = PiRG), overlapping responses for EM-associated genes in mycorrhizal and nonmycorrhizal roots with salt stress (MS/NS = EMAG), and stress-associated genes in nonmycorrhizal roots (NS/NC = STAG) and in mycorrhizal roots (MS/MC = MSAG). ns, Not significantly differentially affected.

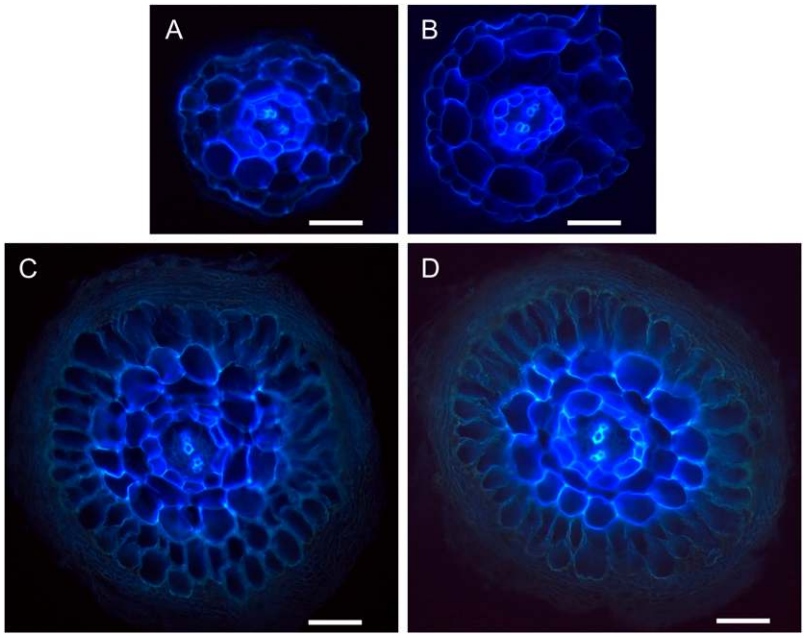

Figure 4. Transverse sections of nonmycorrhizal (A and B) and ectomycorrhizal (C and D) root tips of poplar (*P.* × *canescens*) grown under control conditions (A and C) or in the presence of salt stress (B and D). Sections were viewed with an epifluorescence microscope. Bars = 50 μm.

protein were categories of genes with decreased transcript levels (Fig. 3). Since riboflavin is important for pathogen defense (Zhang et al., 2009), suppression of its biosynthesis may be required to maintain functional EMs.

Mycorrhizas and Salt Stress Induce ABA and SA and Stimulate Carbohydrate Physiology

To distinguish between stress-specific and mycorrhiza-associated responses in EM roots, we exposed mycorrhizal and nonmycorrhizal poplar plants to salt stress. This treatment caused significant accumulation of sodium in roots (Fig. 2D) but had no significant effect on EM colonization (56% ± 2% for EM salt-stressed plants versus 62% ± 2% for EM non-salt-stressed plants; P = 0.1363). The well-known Na^+-induced decreases in potassium were found and compensated the cation balance (Fig. 2D). Other major nutrient elements such as nitrogen and phosphorus were unaffected by excess salinity (Table II). The root system of mycorrhizal plants was better protected from salinity, since the relative loss in fine root biomass was less pronounced than in nonmycorrhizal plants (Table I). With the exception of myoinositol, no influence of salinity on carbohydrates and sugar alcohols was found (Fig. 2, A and B). However, myoinositol increased more strongly in EM than in non-EM roots (Fig. 2B). Glutamate and 4-aminobutyric acid accumulated in response to salinity, whereas other amino compounds were unaffected (Fig. 2C).

Salinity had effects on the signaling metabolites SA, ABA, JA, and auxin similar to those observed under the influence of mycorrhiza: increases in SA and ABA and decreases in JA and auxin (Table III). However, the changes in phytohormone concentrations were stronger with salt than under the influence of EMs and strongest in EM roots exposed to salt stress (Table III).

Stress-Independent Mycorrhiza-Responsive Genes

We used salt-stressed EM and salt-stressed non-EM roots for transcriptome analysis and defined all PiRGs that showed overlapping responses in the combinations MC/NC and MS/NS (see "Materials and Methods") as ectomycorrhiza-associated genes (EMAGs), because these genes were responsive to EMs irrespective of the presence of salt stress. Based on unique gene models, 31 overlapping genes were present under the conditions of MC/NC and MS/NS, for which 24 AGI annotations were obtained (Fig. 3).

Among the EMAGs with increased transcripts were genes encoding glycerinaldehyde-3-phosphate dehydrogenase involved in energy metabolism, a fatty acyl-ACP thioesterase B that is involved in the biosynthesis of C-16 fatty acids, a Δ-8 sphingolipid desaturase that may be involved in vesicle and plasma membrane biosynthesis, three cytochrome P450 oxidases that may catalyze degradation processes of antifungal compounds, such as α-pinene (Loreto et al., 2008), one stress-related gene (Bet v I allergen family), two UDP-glycosyl transferase family proteins of which one may be a flavonol glucosyl transferase, TUBBY-like protein 3 (protein metabolism), cellulose synthase involved in cell wall metabolism, two transporters, and one unknown protein (Fig. 3).

Among the EMAGs with decreased transcript levels in salt-stressed EM roots compared with salt-stressed non-EM roots were genes related to lipid metabolism and transport (PLPζ2 and glycerol-3-phosphate transporter), two acid phosphatases (ACP5 and PAP10), two transcription factors (AS1 and HAP2A), and sig-

naling proteins (inositol-1,3,4-trisphosphate 5/6 kinase and two rho-GTPase-activating proteins; Fig. 3). A gene with a SPX domain displayed decreased transcript level after salt exposure (Fig. 3).

Correlation analysis showed that the relative response of EMAGs under salt stress was only half of that under nonstressed conditions (Fig. 5A). The consistent pattern suggests that these coregulated genes may have crucial roles in maintaining steady-state mycorrhizal functioning.

EMs Activate Genes Involved in the Response to Salinity

Our data indicated that EMs caused permanent activation of stress pathways in roots. Since EM roots contained increased concentrations of carbohydrates and ABA, we speculated that genes related to osmotic stress might be involved. To investigate whether part of the PiRGs are, in fact, members of the osmotic/salinity response of poplar (stress-associated genes [STAGs]), we investigated the root transcriptome under salt stress. In non-EM roots, salinity caused significant changes of 1,452 transcripts, and in EM roots, it caused significant changes of 867 transcripts, corresponding to 993 and 607 genes with unique homologs in Arabidopsis, respectively. These numbers are lower than those found in salt-stressed Arabidopsis roots (Kilian et al., 2007). The difference in responsiveness may be due to the fact that poplar plants were salt exposed for almost 3 weeks, whereas Arabidopsis plants were harvested already after 24 h, when stress acclimation was probably not yet accomplished (Kilian et al., 2007). A detailed analysis of salinity effects on the root transcriptome is beyond the scope of this study and will be presented elsewhere.

Here, we focused on EM-activated genes involved in stress adaptation: these genes must be coexpressed under the conditions of MC/NC and NS/NC. Based on unique gene models, a total number of 29 overlapping genes (STAGs) were identified, for which 27 AGI annotations were obtained (Fig. 3). Two outliers were identified, trypsin/protease inhibitor family protein (Kunitz) and germin-like protein (GLP2), which responded more strongly to salt stress than to EMs. For the other genes, a significant linear regression was obtained with a slope of 0.768, indicating that both salt and EM colonization evoke similar responses (Fig. 5A). The subset of PiRGs that was affected under conditions MS/MC (=MSAG; for mycorrhizal stress-associated genes) and NS/NC (=STAG) was small (Fig. 3). Nevertheless, a significant correlation was found with a flat slope of 0.241 (Fig. 5B). This indicates that mycorrhiza led to dampening of the salt response.

More than half of the identified STAGs were classified under Biotic Stress Responses in MapMan. The list of STAGs with increased transcript levels included galactinol synthase, glycerinaldehyde-3-phosphate dehydrogenase, stress-regulated transcription factors (GASA5, WRKY40, RD26, and TUBBY), two putative signaling proteins (GRF9 and photoassimilate-responsive protein), stress-related genes (glutathione *S*-transferase, DNAJ, germin 2A, two protease inhibitors, and PLP2), and some proteins with unknown functions (Fig. 3). Aldehyde dehydrogenase, signaling proteins (MPK9 and rho-GTPase), pectin methylesterase (cell wall metabolism), and two genes with unknown functions were STAGs with decreased transcript abundances (Fig. 3).

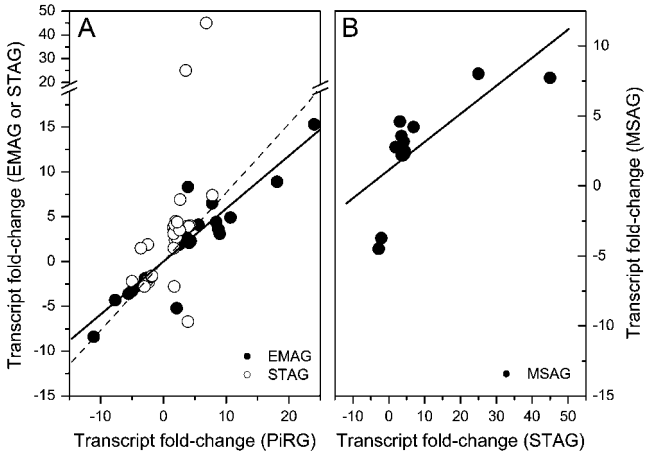

Figure 5. A, Correlation between the relative transcript abundance of *P. involutus* mycorrhiza-responsive genes under control conditions (PiRGs = MC/NC) and mycorrhiza-responsive genes under salt stress (EMAGs = MS/NS = 0.589*x*, $r = 0.919$, $P \leq 0.001$) or with salt-responsive genes in nonmycorrhizal roots (STAGs = NS/NC = 0.768*x*, $r = 0.571$, $P = 0.009$). B, Correlation of salt-responsive genes in nonmycorrhizal (STAG) and mycorrhizal roots (MSAG = MS/MC = 0.241*x*, $r = 0.729$, $P = 0.008$). Data were obtained from Supplemental Tables S2 and S3.

DISCUSSION

EM Roots Display a Shift in the Phytohormone Balance and Hypertrophic Cell Growth

Our genome-wide analysis of transcriptional changes provided clear evidence for reprogramming of cellular differentiation processes by *P. involutus*, since transcription factors involved in developmental processes were repressed and a homolog of cytochrome CYP78A5 (KLUH) that controls organ size in Arabidopsis was increased (Anastasiou et al., 2007). Indeed, these transcriptional changes correlated with strongly increased cell volumes, which occurred specifically where root cells were in contact with the Hartig net (Fig. 1; Table I). The observed hypertrophic cell growth was most likely achieved by coordination of two processes in EMs: (1) increased water uptake driven by elevated concentrations of osmolytes (Fig. 2); and (2) decreased cell wall stiffness mediated by changes in cell wall properties through transcriptional regulation (Fig. 3).

Physiologically, increased carbohydrate concentrations that build up increased osmotic pressure imply stronger sink activity in EM than in non-EM roots. In aerial tissues, ABA application was shown to increase sink strength (Travaglia et al., 2007). Here, we suspect that fungal effectors may activate ABA production in poplar roots, which in turn might have affected sink properties, thereby increasing osmotic potential and affording water uptake and volume increases.

In addition to changes in carbohydrate metabolism, the functioning of EM roots also involved changes in cell wall biosynthesis: transcripts encoding cellulose synthase and an extensin-like protein were increased and those of pectin methylesterase were decreased, which suggests higher cellulose formation and cell wall loosening (Pelloux et al., 2007). Similar observations pointing to cell wall loosening have been reported for EM roots of pine (*Pinus sylvestris*) after infection with *Laccaria bicolor* (Heller et al., 2008). However, a different set of cell wall-associated genes was involved in the pine system compared with *Paxillus-Populus*, suggesting that each fungus-host combination may recruit specific pathways for cell wall modification. In pine, a whole array of genes encoding enzymes of phenolic biosynthesis and polymerization, such as cinnamoyl-CoA reductase, cinnamoyl alcohol dehydrogenase, xyloglucan transendoglucanase, and peroxidase, were suppressed (Heller et al., 2008). Decreases in cell wall phenolics and peroxidase activities have previously been reported in mature conifer mycorrhizas (Münzenberger et al., 1995, 1997). In functional poplar EMs, the cells ensheathed by the Hartig net did not incorporate phenolic compounds, in contrast to the epidermal cells from which they were derived (Fig. 4). Correspondingly, transcripts of a gene encoding a cytochrome P450 reductase (AR1) were suppressed. Causal links between cell wall phenolics and this enzyme still need to be established, but in poplar EM roots, no further obvious transcriptional changes (e.g. of peroxidases or other defense enzymes) were found. This suggests that *P. involutus* affects host cell metabolism by specific inhibition of cell wall phenolics in the contact zone.

The role of auxin in EM formation is unclear and controversial. For example, auxin overproducers of the EM fungus *Hebeloma crustuliniforme* resulted in stronger EM formation, supporting the "auxin hypothesis," which proposes that elevated auxin levels stimulate mycorrhiza formation (Gay et al., 1994; Barker and Tagu, 2000). Most studies with crop plants detected increased auxin concentrations in AM compared with noncolonized roots; however, the effect was time dependent (Fitze et al., 2005; Hause et al., 2007; Jentschel et al., 2007). In contrast to the auxin hypothesis, early work of Wallander et al. (1992) showed that spruce EMs contained decreased auxin levels. Recently, Reddy et al. (2006) found that the auxin-responsive *GH3.16* mRNA was suppressed in EM pine roots. Our data clearly document that in functional mature EMs, auxin was decreased in a tissue-specific manner (Fig. 1; Table III). Transcriptional analysis also supported a massive influence of EMs on auxin metabolism, with suppression of auxin trafficking and auxin- and/or JA-mediated protein degradation via the SCF^{TIR} proteasome (Fig. 3). As auxin triggers the expression of enzymes involved in the biosynthesis of cell wall compounds and is affected by peroxidases (Tognolli et al., 2002; Laskowski et al., 2006), we suggest that decreased auxin levels may be involved in suppressing certain defense pathways involving cell wall stiffening and, thus, enable stable interaction of EM fungi with the host.

However, defense responses are not completely abolished when the plant-fungus association is built up. Transient activation of the phenylpropanoid pathway and strong increases of many defense-related transcripts (e.g. metallothioneins, metallothionein-like proteins, chitinases, and glutathione transferases) were observed in host plants (Franken and Gnädinger, 1994; Johansson et al., 2004; Duplessis et al., 2005; Frettinger et al., 2007; Heller et al., 2008). Although significant, the number of EM-responsive genes in the category Stress was modest in comparison with other studies (Fig. 3). These differences are probably due to the fact that the differentially expressed transcripts in our study reflect host responses to the functioning and maintenance of EMs in the mature stage rather than to the establishment of EMs in the early stage of colonization.

Improved Nutrition in EMs Involves Ammonium Transport Stimulation and Regulation of Phosphorus Uptake

In poplar, association with *P. involutus* ameliorated phosphorus and nitrogen nutrition (Langenfeld-Heyser et al., 2007). Induction of *AMT3;1* points to nitrogen translocation between ectomycorrhizal partners (Chalot et al., 2006), probably resulting in the observed increased free amino acid concentrations in roots (Fig. 2). Selle et al. (2005) showed that an increased ammonium uptake capacity of ectomycorrhizal *P. trichocarpa* roots was realized through mycorrhiza-dependent upregulation of the ammonium transporter *PttAMT1;2*, whereas *AMT3;1* was only overexpressed in senescing leaves (Couturier et al., 2007). Since we double-checked the expression of *AMT3;1* by resequencing the PCR product and by qRT-PCR analysis, we conclude that this transporter is also induced by EMs. However, this may require strong fungal colonization and vigorously growing plants, which might have been prevented in the petri dish system used by Couturier et al. (2007).

In contrast to ammonium transporters, increases in specific phosphate transporters as observed in AM roots (Grunwald et al., 2009) were not detected in this or in other studies with EM fungi (Le Queré et al., 2005; Martin et al., 2008). Acid phosphatases may function in phosphorus mobilization, as they were increased upon phosphorus starvation (del Pozo et al.,

1999). Transcripts for these enzymes were decreased in our study, indicating that acid phosphatases are responding to increased intercellular phosphorus concentrations in EM compared with non-EM roots. Furthermore, transcript abundance of a gene with a SPX/PHOX domain was increased in EM compared with non-EM roots (Fig. 3). The N termini of several members of this family are involved in the regulation of phosphate transport, including the putative phosphate level sensors PHO81 from *Saccharomyces cerevisiae* and NUC-2 from *Neurospora crassa* (Lenburg and O'Shea, 1996; Lee et al., 2000). Genes containing SPX1 domains were also involved in phosphorus sensing and regulation of phosphorus contents in Arabidopsis and rice (*Oryza sativa*; Wang et al., 2004, 2009). In particular, overexpression of the rice enzyme OsSPX1 suppressed *OsPAP10* (for purple acid phosphatase 10) and *OsSQD2* (for sulfoquinovosyldiacylglycerol 2), transcripts of which were also decreased in our study. Earlier studies showed that decreased sulfoquinovosyldiacylglycerol synthesis indicates sufficient phosphate nutrition (Benning, 1998). In addition, transcription phospholipase D2 family protein, a gene with functions in phosphatidic acid accumulation under phosphorus starvation (Li et al., 2006), was also decreased in EM roots. Therefore, collectively, these observations suggest that improved phosphorus supply, evident from phosphorus increases in roots (Table II) and leaves (Langenfeld-Heyser et al., 2007) after long-term EM colonization of poplar, leads to down-regulation of phosphorus-sensing pathways and uptake in roots.

EMs Lead to Activation of Defenses and Prime Roots for Increased Salt Tolerance Involving SA and ABA

Colonization with *P. involutus* protected fine roots against salt-induced biomass loss (Table I). The ability of symbiotic and endophytic fungi to increase salt tolerance has also been reported for other plant species (Feng et al., 2002; Muhsin and Zwiazek, 2002; Waller et al., 2005; Bois et al., 2006). Our study elucidates some of the underlying molecular mechanisms. About one-quarter of the PiRGs showed overlap with salt stress-responsive genes in non-EM roots, which underlines that in functional EMs endogenous plant defense systems are activated. The induction of stress-anticipatory reactions in plants has been called priming (Beckers and Conrath, 2007). Phytohormones play important roles in this respect. For example, systemic acquired resistance, which relies on increased SA levels (Loake and Grant, 2007), MIR, which is thought to be mediated mainly by JA-related pathways (Pozo and Azcon-Aguilar, 2007), and chemical stimulation of ABA production (Jakab et al., 2005) lead to higher resistance of plants to subsequent pathogen or abiotic stresses. A striking difference to MIR that has so far only been studied in AM roots was increased SA and ABA and decreased JA concentrations in EM roots (Table III). This observation suggests that EMs and AMs recruit different signaling pathways to influence plant stress responses.

SA protects plants against abiotic stress involving reactive oxygen species (Koch et al., 2000). This function may be important to prevent injury to EM roots, because the hyphal mantle produces significant amounts of hydrogen peroxide (Gafur et al., 2004). In addition, SA increased in salt-stressed plants (Sawada et al., 2006), where it may counteract negative effects of salt-induced hydrogen peroxide accumulation (Langenfeld-Heyser et al., 2007). As SA levels were higher in salt-stressed EM than in non-EM roots, despite lower endogenous sodium concentrations, we suspect that preactivation of defenses via SA is an important component of EM-induced protection against salinity.

Enhanced SA levels are especially important to reduce the susceptibility of plants to biotic stresses (Shah, 2003). High endogenous SA concentrations prevented colonization of roots with biotrophic fungi (Herrera-Medina et al., 2003; Loake and Grant, 2007). Consistent with this fact is the observation that EM plants generally have higher pathogen resistance than nonmycorrhizal plants (Smith and Read, 2008) and that genes involved in biotic defenses, such as germin-like and Bet v allergen, were activated (Fig. 3). Some transcription and signaling factors activated (TCP transcription factor and WRKY40) or repressed (MPK19 and rho-GTPase-activating protein) by EMs in our study were previously shown to be regulated via BTH [for benzo-(1,2,3)thiadiazole-7-carbothioic acid-*S*-methyl ester], an analog of SA (Wang et al., 2006). BTH has been used commercially as a plant protectant to prime SA-signaling pathways (Beckers and Conrath, 2007). Thus, our study provides evidence that EM-mediated plant protection involves SA.

ABA is a central regulator of plant responses to environmental cues and has also been invoked in biotic interactions (Mauch-Mani and Mauch, 2005). In line with observations that ABA increased susceptibility for biotrophs, colonization of tomato (*Solanum lycopersicum*) with AM fungi (*Glomus intraradices*) increased in plants with elevated ABA levels (Herrera-Medina et al., 2007). As there is evidence that ABA acts against necrotrophic fungi and oomycetes (Ton and Mauch-Mani, 2004; Adie et al., 2007), it may contribute to strengthen pathogen resistance of EM plants. However, the best known functions of ABA are related to the recruitment of stress-signaling networks. ABA accumulates in plants exposed to salt stress (Chen et al., 2003; Chang et al., 2006), and deficiency makes plants more stress sensitive (Xiong et al., 2002). Genevestigator analysis of our PiRGs showed that many stress-related genes were activated by ABA or salt in Arabidopsis (RD26, LPT family protein, aldehyde dehydrogenase 7B4, galactinol synthase, phospholipase 2A, photoassimilate-responsive protein, WRKY40, and glutathione *S*-transferase), whereas a common feature of genes in the category Signaling was that their transcript abundance decreased in response to ABA

(Supplemental Fig. S4). Recently, a novel family of ABA receptors has been identified with high homology to Bet v I allergen family protein that mediates ABA signal transduction by protein phosphatases (Ma et al., 2009). The induction of *Bet v I allergen* transcripts has often been observed upon colonization of plant roots by EM fungi (Johansson et al., 2004; Duplessis et al., 2005; Le Queré et al., 2005; this study). Since the response persisted in EM plants that were salt stressed but did not appear in salt-stressed nonmycorrhizal plants, we conclude that this protein is important for EM interaction but not for triggering ABA responses to salinity.

GOLS2 transcript abundance and Suc and sugar alcohol levels were increased in EM control roots. Accumulation of compatible solutes contributes to protection against osmotic stress, probably as molecular chaperones (Polle et al., 2006). For example, transgenic poplar overaccumulating mannitol displayed increased salt tolerance in comparison with wild-type poplar (Hu et al., 2005). Myoinositol has also been implicated in salt tolerance (Majumder et al., 2003; Das-Chatterjee et al., 2006). Its biosynthesis was increased during salinity stress in common ice plant (*Mesembryanthemum crystallinum*; Ishitani et al., 1996) and in the Arabidopsis-related halophytic salt cress (*Thellungiella halophila*; Taji et al., 2004). Suc and myoinositol play key roles in desiccation protection of resurrection plants (*Craterostigma platagineum*; Peters et al., 2007; Lehner et al., 2008). Induction of galactinol synthase, the entry into the raffinose pathway, was observed in many stress screens (Taji et al., 2002; Jiang and Deyholos, 2006) and was among the few transcripts responsive to environmental stress in the salt-tolerant *Populus euphratica* (Brosché et al., 2005; Ottow et al., 2005). The observed increases in carbohydrate physiology in EM roots indicate a status of stress preparedness. Since accumulation of sugar alcohols was stronger in EM roots exposed to salt stress than in non-EM roots even though sodium accumulation was lower, we conclude that priming of myoinositol biosynthesis belongs to the defense network activated by *P. involutus*. This finding may also be relevant with respect to the maintenance of an improved potassium balance (K^+/Na^+ of 0.6 in EM roots and 0.3 in non-EM roots exposed to salt stress), because compatible solutes can reduce stress-induced potassium efflux (Cuin and Shabala, 2007) and a high K^+-to-Na^+ ratio is crucial for salt tolerance (Munns and Tester, 2008).

In conclusion, our study shows that roots colonized with an EM fungus undergo massive reprogramming leading to changes in cell shape and cell wall properties, probably mediated by a fungal influence on auxin physiology. *P. involutus* induced a novel functional anatomy required for compatible interaction, because phenolic incorporation and rigidification of cell walls was suppressed and because cell volumes in contact with the EM fungus were strongly increased, resembling induced feeding structure. In addition to enabling its accommodation, *P. involutus* also primed roots for increased stress tolerance. This involved upgrading of carbohydrate physiology, activation of stress-responsive genes, and suppression of signaling pathways that are negatively regulated by ABA. In contrast to MIR of AMs, upgrading of roots for improved stress tolerance involved increases in ABA and SA and decreases in JA. Stronger induction of defense pathways and metabolites in EM roots than in non-EM roots exposed to excess salinity indicated that *P. involutus* has the ability to prime plants for increased stress tolerance. Ecologically, it makes sense for the fungus to protect its carbohydrate source. In a wider context, these findings imply that the functioning and maintenance of EM in forests are essential to improve forest tree fitness and that inoculation with EM fungi may be an important measure to ensure biomass production in adverse environments.

MATERIALS AND METHODS

Cultivation of *Paxillus involutus* and Poplar Plants

Paxillus involutus (strain MAJ in the Göttingen stock collection, initially collected in France under a poplar tree) was grown on 2% modified Melin-Norkrans agar medium and subsequently in liquid culture medium as described previously (Langenfeld-Heyser et al., 2007).

Plantlets of *Populus* × *canescens* (=*Populus tremula* × *Populus alba*; clone B1-714) and the lines 31 and 51 transformed with an auxin-responsive GH3::GUS construct as described elsewhere (Teichmann et al., 2008) were multiplied by micropropagation (Leplé et al., 1992). Rooted plantlets of wild-type and transgenic plants were transferred to agar medium in petri dishes and inoculated under axenic conditions with *P. involutus* (Gafur et al., 2004). The plants were cultivated for 3 weeks in a growth room (21°C, 50%–60% relative air humidity, 16 h of light per day, 150 μmol photons m^{-2} s^{-1} photosynthetic active radiation at plant height). Subsequently, the roots were harvested for GUS staining and anatomical analysis.

Mycorrhizal Inoculation, Plant Cultivation, and Salt Exposure

For metabolite and transcriptional analyses, wild-type plantlets of *P.* × *canescens* were multiplied by micropropagation (Leplé et al., 1992). To acclimatize wild-type poplar to ambient conditions, rooted plantlets were cultivated in hydroponic LN nutrient solution (300 μM NH_4NO_3; after Matzner et al., 1982) for 3 weeks in a growth room (21°C, 50%–60% relative air humidity, 16 h of light per day, 150 μmol photons m^{-2} s^{-1} photosynthetic active radiation at plant height) before mycorrhizal inoculation and transfer to climatized cabinets with the same environmental conditions.

Mycelia of *P. involutus* after growth for 4 weeks in liquid culture were used for inoculation. The upper clear supernatant of the culture medium was discarded. Slurry containing mycelia of *P. involutus* was homogenized, and 50 mL was used to inoculate the rooting medium of each plant. The rooting medium, consisting of five parts peat, five parts fine sand (grain size of 0.1–0.3 mm), and 10 parts coarse sand (grain size of 1.2–2.0 mm), was sterilized before inoculation as described elsewhere (Luo et al., 2009). For plant cultivation, growth tubes (5 cm diameter, 41 cm height) with a nylon mesh at the bottom were filled with inoculated or noninoculated rooting medium. Subsequently, 74 wild-type poplar plantlets were planted in 74 growth tubes. The plants were randomized twice per week. Each plant was irrigated daily with 20 mL of sterile LN nutrient solution in the morning and 20 mL of sterile water in the evening. Poplar plants were grown in the climatized room for 13 weeks. Before starting salt stress treatment, some plants were harvested and used to control mycorrhizal colonization. Half of the plants of each treatment (i.e. mycorrhizal plants [M] and noninoculated controls [N]) were irrigated either with LN nutrient solution once per day (NC, MC) or with LN nutrient solution containing additionally 150 mM NaCl (NS, MS).

Harvest

After 18 d of salt exposure, all plants were harvested. The plants were separated into leaves, stems, and coarse and fine roots. Subsamples of fine roots for microscopic investigations were transferred into FAE solution (37% formalin:glacial acetic acid:70% ethyl alcohol = 5:5:90; Luo et al., 2005).

For biochemical and molecular analyses, fresh tissues were immediately frozen in liquid nitrogen and subsequently stored at –80°C. Frozen samples were milled to a fine powder with a ball mill (Retsch) precooled in liquid nitrogen. Aliquots of plant powder were dried for 48 h at 60°C and used for determination of the fresh-to-dry mass ratio. For the determination of nutrient elements, carbohydrates, and phytohormones in fine roots, equal weights of fine root powder from four harvested plants within each treatment were pooled. Four independent biological replicates were used for the analyses.

Microscopic Investigation of Roots and EMs

Subsamples of fine roots were taken from the root systems of *P.* × *canescens* from each treatment (NC, NS, MC, MS). The subsamples were spread in petri dishes with water and examined with a binocular microscope (Stemi SV11; Zeiss) for ectomycorrhizal root tips. The degree of ectomycorrhization was calculated based on the amount of ectomycorrhizal root tips per 100 root tips for 16 samples per treatment.

Roots of wild-type and transgenic lines were stained in darkness with 5-bromo-4-chloro-3-indole-D-GlcUA (Duchefa) for 24 h at 37°C (Teichmann et al., 2008). Mycorrhizal and nonmycorrhizal roots of all experiments were embedded for light microscopy (Teichmann et al., 2008). Transverse and longitudinal sections of fine roots and mycorrhizas (40 μm thickness) were cut with a freezing microtome (Reichert-Jung, Cambridge Instruments), examined, and photographed with a light microscope (Axioskop; Zeiss) with a digital camera (AxioCam MRc; Carl Zeiss MicroImaging) connected to a computer (AxioVision Rel. 4.6; Carl Zeiss Canada).

Cross sections of mycorrhizal and nonmycorrhizal roots were also mounted in 70% glycerol and observed with an epifluorescence microscope (Axioplan; Zeiss) using the Zeiss filter combination G 365, FT 395, and LP 420, and micrographs were taken as above.

Element Analysis

Dry fine roots were ball milled to a fine powder and used for analysis of elements. After extraction with HNO_3, mineral elements were determined by an inductively coupled plasma-atomic emission spectrometer (Spectroflame; Spectro Analytical Instruments) as described by Heinrichs et al. (1986). Nitrogen and carbon were determined using a C/N analyzer (Elemental Analyzer EA1108; Carlo Erba Strumentazione).

Determination of Sugars and Sugar Alcohols

The soluble sugars and sugar alcohols in fine roots were determined by gas chromatography-mass spectrometry (GC-MS) as described by Hu et al. (2005). Briefly, about 50 mg of frozen-dried materials from each pooled sample was extracted in 500 μL of extraction solution (methanol:chloroform:water, 12:5:3, v/v/v), and the extracted products were acetylation derivatized and then separated in a DB-17 capillary column (30 m × 0.25 mm × 0.25 μm; J&W Scientific) attached to a Finnigan Trace GC ultra and quantified with a Finnigan Trace GC ultra-Trace DSQ GC-MS system (Thermo Electron). Ribitol was used as the internal standard in the analysis, and mannitol, Gal, sorbitol, Fru, myoinositol, Glc, Suc, and trehalose were used as standards to identify and quantify the concentrations of sugars and sugar alcohols.

Determination of Phytohormones

Phytohormones were extracted after Matyash et al. (2008) with some modifications. Plant material (500 mg) was extracted with 0.75 mL of methanol containing 10 ng of D_6-SA, 10 ng of D_6-ABA (both from CDN Isotopes), 10 ng of D_6-JA, 30 ng of D_5-oPDA, 10 ng of D_4-JA-Leu (all three kindly provided by Otto Miersch), and 10 ng of D_5-IAA (Eurisotop) each as internal standard. After mixing, 2.5 mL of methyl-*tert*-butyl ether was added and the extract was shaken for 1 h at room temperature. For phase separation, 0.625 mL of water was added. The mixture was incubated for 10 min at room temperature and centrifuged at 450*g* for 15 min. The upper phase was collected and the lower phase was reextracted with 0.7 mL of methanol and 1.3 mL of methyl-*tert*-butyl ether as described above. The combined upper phases were dried under streaming nitrogen and resuspended in 100 μL of acetonitrile:water:acetic acid (20:80:0.1, v/v/v).

The analysis of constituents was performed using an Agilent 1100 HPLC system coupled to an Applied Biosystems 3200 hybrid triple quadrupole/linear ion-trap mass spectrometer (MDS Sciex). Nanoelectrospray (nanoESI) analysis was achieved using a chip ion source (TriVersa NanoMate; Advion BioSciences). Reverse-phase HPLC separation was performed on an EC 50/2 Nucleodure C18 gravity 1.8 μm column (50 × 2 mm, 1.8 μm particle size; Macherey-Nagel). The binary gradient system consisted of solvent A (acetonitrile:water:acetic acid, 20:80:0.1 [v/v/v]) and solvent B (acetonitrile:acetic acid, 100:0.1 [v/v]) with the following gradient program: 10% solvent B for 2 min, followed by a linear increase of solvent B up to 90% within 6 min and an isocratic run at 90% solvent B for 2 min. The flow rate was 0.3 mL min^{-1}. For stable nanoESI, 50 μL min^{-1} 2-propanol:acetonitrile:water:formic acid (70:20:10:0.1, v/v/v/v) delivered by a 515 HPLC pump (Waters) was added just after the column via a mixing T valve. Using another postcolumn splitter, 740 nL min^{-1} of the eluent was directed to the nanoESI chip. Ionization voltage was set to −1.7 kV. Phytohormones were ionized in a negative mode and determined in multiple reaction monitoring mode. Mass transitions were as follows: 141/97 (declustering potential [DP] −45 V, entrance potential [EP] −7 V, collision energy [CE] −22 V) for D_6-SA, 137/93 (DP −45 V, EP −7 V, CE −22 V) for SA, 179/135 (DP −40 V, EP −6.5 V, CE −22 V) for D_5-IAA, 174/130 (DP −40 V, EP −6.5 V, CE −22 V) for IAA, 215/59 (DP −45 V, EP −9.5 V, CE −22 V) for D_6-JA, 209/59 (DP −45 V, EP −9.5 V, CE −22 V) for JA, 269/159 (DP −55 V, EP −9 V, CE −16 V) for D_6-ABA, 263/153 (DP −55 V, EP −9 V, CE −16 V) for ABA, 296/170 (DP −70 V, EP −8.5 V, CE −28 V) for D_5-oPDA, 291/165 (DP −70 V, EP −8.5 V, CE −28 V) for oPDA, 263/59 (DP −70 V, EP −8.5 V, CE −28 V) for dinor-oPDA, 325/133 (DP −80 V, EP −4 V, CE −30 V) for D_4-JA-Leu, and 322/130 (DP −80 V, EP −4 V, CE −30 V) for JA-Ile. The mass analyzers were adjusted to a resolution of 0.7 atomic mass unit full width at half height. The ion source temperature was 40°C, and the curtain gas was set at 10 (given in arbitrary units). Quantification was carried out using a calibration curve of intensity (mass-to-charge ratio) of unlabeled/deuterium labeled versus molar amounts of unlabeled (0.3–1,000 pmol).

Determination of Fatty Acids

For determination of the fatty acids in fine roots of *P.* × *canescens*, preparation of methyl esters of fatty acids for analysis by GC-flame ionization detection was performed according to the method of Miquel and Browse (1992). For acidic hydrolysis, 1 mL of a methanolic solution containing 2.75% (v/v) H_2SO_4 (95%–97%) and 2% (v/v) dimethoxypropan was added to 10 mg of sample. For later quantification of the fatty acids, 5 μg of triheptadecanoate was added and the sample was incubated for 1 h at 80°C. To extract the resulting methyl esters of fatty acids, 200 μL of saturated aqueous NaCl solution and 2 mL of hexane were added. The hexane phase was dried under streaming nitrogen and redissolved with equal volumes of water and hexane. The hexane phase was filtered with cotton wool soaked with $NaSO_4$ and dried under streaming nitrogen. Finally, the sample was redissolved in 10 μL of acetonitrile for GC analysis performed with an Agilent 6890 gas chromatograph fitted with a capillary DB-23 column (30 m × 0.25 mm; 0.25 μm coating thickness; J&W Scientific, Agilent). Helium was used as carrier gas at a flow rate of 1 mL min^{-1}. The temperature gradient was 150°C for 1 min, 150°C to 200°C at 8 K min^{-1}, 200°C to 250°C at 25 K min^{-1}, and 250°C for 6 min.

Determination of Amino Compounds

For determination of amino compounds in fine roots of *P.* × *canescens*, approximately 0.1 g of homogenized material was extracted according to the method of Winter et al. (1992). Subsequently, the extract was freeze dried and resuspended in 1 mL of 0.02 M HCl prior to derivatization. For derivatization, 5 μL of the resuspended extracts was mixed with 35 μL of AccQ-Tag Ultra Borate buffer and 10 μL of AccQ-Tag Reagent (Waters). The samples were derivatized for 10 min at 55°C after incubation for 1 min at room temperature. To account for the difference in the efficiency of derivatization, an internal standard (Norvaline; 10 μM in total derivatization reaction) was added to the AccQ-Tag Ultra Borate buffer. For analysis of the compositions and concentrations of amino compounds, a Waters Acquity UPLC-System using an AccQ-Tag Ultra column (2.1 × 100 mm; Waters) was employed. A 1-μL sample was injected and separated by gradually changing the composition of the two

eluents, Waters AccQ-Tag Ultra Eluent A and B (Waters), from 99.9% eluent A/0.1% eluent B to 40.4% eluent A/59.6% eluent B at flow rate of 0.7 mL min^{-1} at 61°C column temperature. The A_{260} was measured. Standard H of amino compounds (NCI0180; Pierce Biotechnology) was used as an analytical standard. Additional standards of amino compounds were added (at 2.5 μmol in 0.1 M HCl each) according to the composition of analyzed samples.

RNA Isolation and DNA Chip Hybridization

Within each treatment, equal weight of fine root powder from four harvested plants of *P.* × *canescens* was pooled. Three independent biological replicates (i.e. 12 plants per treatment) were analyzed per treatment. Total RNA was isolated from about 1 g of fine roots according to the method of Chang et al. (1993) with minor modification. No spermidine was applied in the extraction buffer, and 2% β-mercaptoethanol was used. An additional extraction step was performed after precipitation with 2.5 M LiCl. Total RNA was purified according to the RNeasy mini protocol (Qiagen). The purity and integrity of RNA were assessed according to the Affymetrix GeneChip expression analysis protocol (http://www.affymetrix.com/support/downloads/manuals/expression_analysis_technical_manual.pdf). Further processing of the RNA and complementary RNA hybridization using the Affymetrix poplar genome array were accomplished at the microarray facilities of Eberhard Karls University (http://www.microarray-facility.com/). For each treatment, three arrays were hybridized, thus yielding 12 arrays. The raw data are available under accession number E-MEXP-1874 at the ArrayExpress depository (http://www.ebi.ac.uk/microarray-as/aer/entry;jsessionid=50F7A8619BE733EB58BD0C5F3E3CF8F7).

qRT-PCR Analysis

A subset of six genes was used to validate the microarray results. The primers were designed using open access software (Primer3; http://frodo.wi.mit.edu/cgi-bin/primer3/primer3_www.cgi) and are given in Supplemental Table S5.

Five micrograms of total RNA was digested with deoxyribonuclease from the TURBO DNA-free kit (Ambion) according to the manufacturer's instructions. The success of DNA-free treatment was evaluated by a control real-time PCR. The RNAs after DNA-free treatment were reverse transcribed with Moloney murine leukemia virus reverse transcriptase from the first-strand cDNA synthesis kit (K1612; Fermentas) according to the instructions of the manufacturer. The relative transcript abundance was detected by the MyiQ Single-Color Real-Time PCR Detection System from Bio-Rad using tested primer pairs and SYBR Green PCR Master Mix (Absolute QPCR Mixes; Abgene) according to the manufacturer's instructions. Cycling conditions were 95°C for 1 min, melting temperature for 1 min, and 72°C for 30 s. Our preliminary experiments indicated that both genes ACT2 and 18S were quite stable under current experimental conditions. Thus, ACT2 and 18S were used as internal controls, and a standard curve was established by a series of dilutions. Relative expression ratios of analyzed genes were determined using the relative expression software tool REST (Pfaffl et al., 2002).

Statistical Analysis and Functional Categorization

Statistical tests with physiological and biochemical data were performed with Statgraphics (STN). When interactions were significant, a posteriori comparison of means was done. To reduce the chance of type I errors, all *P* values of the multiple comparisons were corrected by Tukey's honestly significant difference method. Data were tested for normality with the Shapiro-Wilk's test. Differences between parameter means were considered significant when the *P* value of the ANOVA *F*-test was less than 0.05.

For gene expression analysis, the Affymetrix CEL files generated at the Microarray Service Facilities containing the raw probe intensity values from 12 arrays were imported into R (http://www.r-project.org), and further analysis was computed in R. The data were normalized by the quantile normalization method and adjusted for background correction using the robust multiarray average method (Irizarry et al., 2003). Statistical analysis of significantly differentially regulated genes was accomplished using SAM (for significance analysis of microarrays) according to Tusher et al. (2001). SAM assigned a score to each gene on the basis of the change in gene expression relative to the SD of repeated measurements. For genes with scores greater than an adjustable threshold, SAM applied permutations of the repeated measurements to estimate the percentage of genes identified by chance (i.e. the false discovery rate). The false discovery rates were 8.6%, 6.6%, 5.7%, and 6.5% for the comparison conditions of MC/NC, MS/NS, NS/NC, and MS/MC, respectively. The list containing differentially expressed genes was annotated using a database (http://popgenome.ag.utk.edu/mdb/N_Affy_annot.php) and categorized into functional groups using MapMan (version 3.0 ORC1), which was downloaded from the Web site (http://gabi.rzpd.de/projects/MapMan/). For functional group analysis, the AGI number of each corresponding poplar gene was used and entered into MapMan for mapping. Functional categories were determined according to the standard protocol (http://gabi.rzpd.de/projects/MapMan/MapManGuide.pdf). *P* values of functional groups were obtained by Wilcoxon rank sum test in MapMan.

Supplemental Data

The following materials are available in the online version of this article.

Supplemental Figure S1. Correlation between fold changes of gene expression detected by Affymetrix poplar genome array and by qRT-PCR.

Supplemental Figure S2. MapMan visualization of biotic stress pathways with up- and down-regulated genes in mycorrhizal compared with nonmycorrhizal roots.

Supplemental Figure S3. Alignments of ammonium transporter (AMT3.1) at the cDNA and amino acid levels between *P. trichocarpa* and *P.* × *canescens*.

Supplemental Figure S4. Genevestigator analyses of PiRGs with AGI annotations that showed increased (A) or decreased (B) transcript levels.

Supplemental Table S1. Genes with significantly changed transcript abundance in EM compared with non-EM poplar roots.

Supplemental Table S2. AGI annotations of genes with significantly increased transcript abundance in EM compared with non-EM poplar roots.

Supplemental Table S3. AGI annotations of genes with significantly decreased transcript abundance in EM compared with non-EM poplar roots.

Supplemental Table S4. Concentrations of fatty acids in mycorrhizal (M) or nonmycorrhizal (N) fine roots of *P.* × *canescens* grown under control conditions (C) or exposed to salt stress (S).

Supplemental Table S5. Primers used for qRT-PCR.

ACKNOWLEDGMENTS

We are grateful to C. Kettner and S. Elend (Büsgen-Institut) and to P. Meyer, S. Freitag, and A. Mumdey (Albrecht-von-Haller Institute for Plant Sciences) for excellent technical assistance. We thank T. Klein (Labor für Radioisotope, Universität Göttingen) for help with the qRT-PCR and Dr. M. Walter at the microarray facilities of Eberhard Karls Universität for microarray hybridization.

Received June 27, 2009; accepted October 4, 2009; published October 7, 2009.

LITERATURE CITED

Adie BAT, Perez-Perez J, Perez-Perez MM, Godoy M, Sanchez-Serrano JJ, Schmelz EA, Solano R (2007) ABA is an essential signal for plant resistance to pathogens affecting JA biosynthesis and the activation of defenses in *Arabidopsis*. Plant Cell **19:** 1665–1681

Anastasiou E, Kenz S, Gerstung M, MacLean D, Timmer J, Fleck C, Lenhard M (2007) Control of plant organ size by *KLUH/CYP78A5*-dependent intercellular signaling. Dev Cell **13:** 843–856

Barker S, Tagu D (2000) The roles of auxins and cytokinins in mycorrhizal symbioses. J Plant Growth Regul **19:** 144–154

Beckers GJM, Conrath U (2007) Priming for stress resistance: from the lab to the field. Curr Opin Plant Biol **10:** 425–431

Benning C (1998) Biosynthesis and function of the sulfolipid sulfoquinovosyl diacylglycerol. Annu Rev Plant Physiol Plant Mol Biol **49:** 53–75

Bogeat-Triboulot MB, Bartoli F, Garbaye J, Marmeisse R, Tagu D (2004) Fungal ectomycorrhizal community and drought affect root hydraulic properties and soil adherence to roots of *Pinus pinaster* seedlings. Plant Soil **267:** 213–223

Bois G, Bigras F, Bertrand A, Piche Y, Fung MYP, Khasa DP (2006) Ectomycorrhizal fungi affect the physiological responses of *Picea glauca* and *Pinus banksiana* seedlings exposed to an NaCl gradient. Tree Physiol **26:** 1185–1196

Bolu WO, Polle A (2004) Growth and stress reactions in roots and shoots of a salt-sensitive poplar species (*Populus* × *canescens*). Trop Ecol **45:** 161–171

Brosché M, Vinocur B, Alatalo ER, Lamminmäki A, Teichmann T, Ottow EA, Djilianov D, Afif D, Bogeat-Triboulot MB, Altman A, et al (2005) Gene expression and metabolite profiling of *Populus euphratica* growing in the Negev desert. Genome Biol **6:** R101

Chalot M, Blaudez D, Brun A (2006) Ammonia: a candidate for nitrogen transfer at the mycorrhizal interface. Trends Plant Sci **11:** 263–266

Chang S, Puryear J, Cairney J (1993) A simple and efficient method for isolating RNA from pine trees. Plant Mol Biol Rep **11:** 113–116

Chang Y, Chen SL, Yin WL, Wang RG, Liu YF, Shi Y, Shen YY, Li Y, Jiang J, Liu Y (2006) Growth, gas exchange, abscisic acid, and calmodulin response to salt stress in three poplars. J Integr Plant Biol **48:** 286–293

Chen SL, Li JK, Wang TH, Wang SS, Polle A, Huttermann A (2003) Gas exchange, xylem ions and abscisic acid response to Na^+-salts and Cl^--salts in *Populus euphratica*. Acta Bot Sin **45:** 561–566

Couturier J, Montanini B, Martin F, Brun A, Blaudez D, Chalot M (2007) The expanded family of ammonium transporters in the perennial poplar plant. New Phytol **174:** 137–150

Cuin TA, Shabala S (2007) Compatible solutes reduce ROS-induced potassium efflux in *Arabidopsis* roots. Plant Cell Environ **30:** 875–885

Das-Chatterjee A, Goswami L, Maitra S, Dastidar KG, Ray S, Majumder AL (2006) Introgression of a novel salt-tolerant L-myo-inositol 1-phosphate synthase from *Porteresia coarctata* (Roxb.) Tateoka (*PcINO1*) confers salt tolerance to evolutionary diverse organisms. FEBS Lett **580:** 3980–3988

del Pozo JC, Allona I, Rubio V, Leyva A, de la Pena A, Aragoncillo C, Paz-Ares J (1999) A type 5 acid phosphatase gene from *Arabidopsis thaliana* is induced by phosphate starvation and by some other types of phosphate mobilising/oxidative stress conditions. Plant J **19:** 579–589

Duplessis S, Courty PE, Tagu D, Martin F (2005) Transcript patterns associated with ectomycorrhiza development in *Eucalyptus globulus* and *Pisolithus microcarpus*. New Phytol **165:** 599–611

Edeling MA, Smith C, Owen D (2006) Life of a clathrin coat: insights from clathrin and AP structures. Nat Rev Mol Cell Biol **7:** 32–44

Ehlting B, Dluzniewska P, Dietrich H, Selle A, Teuber M, Hansch R, Nehls U, Polle A, Schnitzler JP, Rennenberg H, et al (2007) Interaction of nitrogen nutrition and salinity in grey poplar (*Populus tremula* × *alba*). Plant Cell Environ **30:** 796–811

Feng G, Zhang FS, Li XL, Tian CY, Tang C, Rengel Z (2002) Improved tolerance of maize plants to salt stress by arbuscular mycorrhiza is related to higher accumulation of soluble sugars in roots. Mycorrhiza **12:** 185–190

Fitze D, Wiepning A, Kaldorf M, Ludwig-Müller J (2005) Auxins in the development of an arbuscular mycorrhizal symbiosis in maize. J Plant Physiol **162:** 1210–1219

Franken P, Gnädinger F (1994) Analysis of parsley arbuscular endomycorrhiza: infection development and mRNA levels of defense related genes. Mol Plant Microbe Interact **34:** 241–256

Frettinger P, Derory J, Herrmann S, Plomion C, Lapeyrie F, Oelmüller R, Martin F, Buscot F (2007) Transcriptional changes in two types of pre-mycorrhizal roots and in ectomycorrhizas of oak microcuttings inoculated with *Piloderma croceum*. Planta **225:** 331–340

Gafur A, Schützendübel A, Langenfeld-Heyser R, Fritz E, Polle A (2004) Compatible and incompetent *Paxillus involutus* isolates for ectomycorrhiza formation in vitro with poplar (*Populus* × *canescens*) differ in H_2O_2 production. Plant Biol **6:** 91–99

Gay G, Normand L, Marmeisse R, Sotta B, Debaud JC (1994) Auxin overproducer mutants of *Hebeloma cylindrosporum* Romagnesi have increased mycorrhizal activity. New Phytol **128:** 645–657

Grunwald U, Guo W, Fischer K, Isayenkov S, Ludwig-Müller J, Hause B, Yan X, Küster H, Franken P (2009) Overlapping expression patterns and differential transcript levels of phosphate transporter genes in arbuscular mycorrhizal, Pi-fertilised and phytohormone-treated *Medicago truncatula* roots. Planta **229:** 1023–1034

Hause B, Mrosk C, Isayenkov S, Strack D (2007) Jasmonates in arbuscular mycorrhizal interactions. Phytochemistry **68:** 101–110

Heidtman M, Chen CZ, Collins RN, Barlowe C (2005) Yos1p is a novel subunit of the Yip1p-Yif1p complex and is required for transport between the endoplasmic reticulum and the Golgi complex. Mol Biol Cell **16:** 1673–1683

Heinrichs H, Brumsack HJ, Loftfield N, König N (1986) Verbessertes Druckaufschlussystem für biologische und anorganische Materialien. Z Pflanzenernaehr Bodenkd **149:** 350–353

Heller G, Adomas A, Li G, Osborne J, van Zyl L, Sederoff R, Finlay RD, Stenlid J, Asiegbu FO (2008) Transcriptional analysis of *Pinus sylvestris* roots challenged with the ectomycorrhizal fungus *Laccaria bicolour*. BMC Plant Biol **8:** 19

Herrera-Medina MJ, Gagnon H, Piche Y, Ocampoa JA, Garrido JMG, Vierheilig H (2003) Root colonization by arbuscular mycorrhizal fungi is affected by the salicylic acid content of the plant. Plant Sci **164:** 993–998

Herrera-Medina MJ, Steinkellner S, Vierheilig H, Ocampo Bote JA, García Garrido JM (2007) Abscisic acid determines arbuscule development and functionality in tomato arbuscular mycorrhiza. New Phytol **175:** 554–564

Hu L, Lu H, Liu Q, Chen X, Jiang X (2005) Overexpression of mtlD gene in transgenic *Populus tomentosa* improves salt tolerance through accumulation of mannitol. Tree Physiol **25:** 1273–1281

Irizarry RA, Hobbs B, Collin F, Beazer-Barclay YD, Antonellis KJ, Scherf U, Speed TP (2003) Exploration, normalization, and summaries of high density oligonucleotide array probe level data. Biostatistics **4:** 249–264

Ishitani M, Majumder AL, Bornhouser A, Michalowski CB, Jensen RG, Bohnert HJ (1996) Coordinate transcriptional induction of myo-inositol metabolism during environmental stress. Plant J **9:** 537–548

Jakab G, Ton J, Flors V, Zimmerli L, Metraux JP, Mauch-Mani B (2005) Enhancing *Arabidopsis* salt and drought stress tolerance by chemical priming for its abscisic acid responses. Plant Physiol **139:** 267–274

Jentschel K, Thiel D, Rehn F, Ludwig-Müller J (2007) Arbuscular mycorrhiza enhances auxin levels and alters auxin biosynthesis in *Tropaeolum majus* during early stages of colonization. Physiol Plant **129:** 320–333

Jiang YQ, Deyholos MK (2006) Comprehensive transcriptional profiling of NaCl-stressed *Arabidopsis* roots reveals novel classes of responsive genes. BMC Plant Biol **6:** 20

Johansson T, Le Quere A, Ahren D, Soderstrom B, Erlandsson R, Lundeberg J, Uhlen M, Tunlid A (2004) Transcriptional responses of *Paxillus involutus* and *Betula pendula* during formation of ectomycorrhizal root tissue. Mol Plant Microbe Interact **17:** 202–215

Kilian J, Whitehead D, Horak J, Wanke D, Weinl S, Batistic O, D'Angelo C, Bornberg-Bauer E, Kudla J, Harter K (2007) The AtGenExpress global stress expression data set: protocols, evaluation and model data analysis of UV-B light, drought and cold stress responses. Plant J **50:** 347–363

Koch JR, Creelman RA, Eshita SM, Seskar M, Mullet J, Davis KR (2000) Ozone sensitivity in hybrid poplar correlates with insensitivity to both salicylic acid and jasmonic acid: the role of programmed cell death in lesion formation. Plant Physiol **123:** 487–496

La Camera S, Balague C, Göbel C, Geoffroy P, Legrand M, Feussner I, Roby D, Heitz T (2009) The *Arabidopsis* patatin-like protein 2 (PLP2) plays an essential role in cell death execution and differentially affects biosynthesis of oxylipins and resistance to pathogens. Mol Plant Microbe Interact **22:** 469–481

La Camera S, Geoffroy P, Samaha H, Ndiaye A, Rahim G, Legrand M, Heitz T (2005) A pathogen-inducible patatin-like lipid acyl hydrolase facilitates fungal and bacterial host colonization in *Arabidopsis*. Plant J **44:** 810–825

Langenfeld-Heyser R, Gao J, Ducic T, Tachd P, Lu CF, Fritz E, Gafur A, Polle A (2007) *Paxillus involutus* mycorrhiza attenuate NaCl-stress responses in the salt-sensitive hybrid poplar *Populus* × *canescens*. Mycorrhiza **17:** 121–131

Laskowski M, Biller S, Stanley K, Kajstura T, Prusty P (2006) Expression profiling of auxin-treated *Arabidopsis* roots: toward a molecular analysis of lateral root emergence. Plant Cell Physiol **47:** 788–792

Lee M, O'Regan S, Moreau JL, Johnson AL, Johnston LH, Goding CR (2000) Regulation of the Pcl7-Pho85 cyclin-cdk complex by Pho81. Mol Microbiol **38:** 411–422

Lehner A, Chopera DR, Peters SW, Keller F, Mundree SG, Thomson JA, Farrant JM (2008) Protection mechanisms in the resurrection plant *Xerophyta viscosa*: cloning, expression, characterisation and role of XvINO1, a gene coding for a myo-inositol 1-phosphate synthase. Funct Plant Biol **35:** 26–39

Lenburg ME, O'Shea EK (1996) Signaling phosphate starvation. Trends Biochem Sci **21:** 383–387

Leplé JC, Brasileiro ACM, Michel MF, Delmotte F, Jouanin L (1992) Transgenic poplars: expression of chimeric genes using 4 different constructs. Plant Cell Rep **11:** 137–141

Le Queré A, Wright DP, Soderstrom B, Tunlid A, Johansson T (2005) Global patterns of gene regulation associated with the development of ectomycorrhiza between birch (*Betula pendula* Roth.) and *Paxillus involutus* (Batsch) Fr. Mol Plant Microbe Interact **18:** 659–673

Li G, Xue HW (2007) *Arabidopsis* PLD zeta 2 regulates vesicle trafficking and is required for auxin response. Plant Cell **19:** 281–295

Li MY, Qin CB, Welti R, Wang X (2006) Double knockouts of phospholipases D zeta 1 and D zeta 2 in Arabidopsis affect root elongation during phosphate-limited growth but do not affect root hair patterning. Plant Physiol **140:** 761–770

Liu J, Maldonado-Mendoza I, Lopez-Meyer M, Cheung F, Town CD, Harrison MJ (2007) Arbuscular mycorrhizal symbiosis is accompanied by local and systemic alterations in gene expression and an increase in disease resistance in the shoots. Plant J **50:** 529–544

Loake G, Grant M (2007) Salicylic acid in plant defence: the players and protagonists. Curr Opin Plant Biol **10:** 466–472

Loreto F, Kesselmeier J, Schnitzler JP (2008) Volatile organic compounds in the biosphere-atmosphere system. Plant Biol **10:** 2–7

Ludwig-Müller J (2000) Hormonal balance in plants during colonization by mycorrhizal fungi. *In* Y Kapulnik, D Douds, eds, Arbuscular Mycorrhizas: Physiology and Function. Kluwer Academic Publishers, Amsterdam, pp 263–283

Luo ZB, Langenfeld-Heyser R, Calfapietra C, Polle A (2005) Influence of free air CO_2 enrichment (EUROFACE) and nitrogen fertilisation on the anatomy of juvenile wood of three poplar species after coppicing. Trees (Berl) **19:** 109–118

Luo ZB, Li K, Jiang X, Polle A (2009) The ectomycorrhizal fungus (*Paxillus involutus*) and hydrogels affect drought tolerance of *Populus euphratica*. Ann For Sci **66:** 106

Ma Y, Szostkiewicz I, Korte A, Moes D, Yang Y, Christmann A, Grill E (2009) Regulators of PP2C phosphatase activity function as abscisic acid sensors. Science **324:** 1064–1068

Majumder AL, Chatterjee A, Ghosh Dastidar K, Majee M (2003) Diversification and evolution of L-myo-inositol 1-phosphate synthase. FEBS Lett **553:** 3–10

Martin F, Aerts A, Ahrén D, Brun A, Duchaussoy F, Kohler A, Lindquist E, Salamov A, Shapiro HJ, Wuyts J, et al (2008) The genome sequence of the basidiomycete fungus *Laccaria bicolor* provides insights into the mycorrhizal symbiosis. Nature **452:** 88–92

Martin F, Kohler A, Duplessis S (2007) Living in harmony in the wood underground: ectomycorrhizal genomics. Curr Opin Plant Biol **10:** 204–210

Matyash V, Liebisch G, Kurzchalia TV, Shevchenko A, Schwudke D (2008) Lipid extraction by methyl-tert-butyl ether for high-throughput lipidomics. J Lipid Res **49:** 1137–1146

Matzner E, Khanna P, Meiwes K, Lindheim M, Prenzel J, Ulrich B (1982) Elementflüsse in Waldökosystemen im Solling: Datendokumentation. Göttingen Bodenkundliche Berichte **71:** 1–27

Mauch-Mani B, Mauch F (2005) The role of abscisic acid in plant-pathogen interactions. Curr Opin Plant Biol **8:** 409–414

Miquel M, Browse J (1992) *Arabidopsis* mutants deficient in polyunsaturated fatty acid synthesis. J Biol Chem **267:** 1502–1509

Mizutani M, Ohta D (1998) Two isoforms of NADPH:cytochrome P450 reductase in *Arabidopsis thaliana*: gene structure, heterologous expression in insect cells, and differential regulation. Plant Physiol **116:** 357–367

Morel M, Jacob C, Kohler A, Johansson T, Martin F, Chalot M, Brun A (2005) Identification of genes differentially expressed in extraradical mycelium and ectomycorrhizal roots during *Paxillus involutus-Betula pendula* ectomycorrhizal symbiosis. Appl Environ Microbiol **71:** 382–391

Muhsin TM, Zwiazek JJ (2002) Colonization with *Hebeloma crustuliniforme* increases water conductance and limits shoot sodium uptake in white spruce (*Picea glauca*) seedlings. Plant Soil **238:** 217–225

Munns R, Tester M (2008) Mechanisms of salinity tolerance. Annu Rev Plant Biol **59:** 651–681

Münzenberger B, Kottke I, Oberwinkler F (1995) Reduction of phenolics in mycorrhizas of *Larix decidua* Mill. Tree Physiol **15:** 191–196

Münzenberger B, Otter T, Wüstrich D, Polle A (1997) Peroxidase and laccase activities in mycorrhizal and non-mycorrhizal roots of Norway spruce (*Picea abies* L.) and larch (*Larix decidua*). Can J Bot **75:** 932–938

Nehls U (2008) Mastering ectomycorrhizal symbiosis: the impact of carbohydrates. J Exp Bot **59:** 1097–1108

Ottow EA, Brinker M, Teichmann T, Fritz E, Kaiser W, Brosche M, Kangasjarvi J, Jiang XN, Polle A (2005) *Populus euphratica* displays apoplastic sodium accumulation, osmotic adjustment by decreases in calcium and soluble carbohydrates, and develops leaf succulence under salt stress. Plant Physiol **139:** 1762–1772

Pelloux J, Rustérucci C, Mellerowicz EJ (2007) New insights into pectin methylesterase structure and function. Trends Plant Sci **12:** 267–277

Peters S, Mundree SG, Thomson JA, Farrant JM, Keller F (2007) Protection mechanisms in the resurrection plant *Xerophyta viscosa* (Baker): both sucrose and raffinose family oligosaccharides (RFOs) accumulate in leaves in response to water deficit. J Exp Bot **58:** 1947–1956

Pfaffl MW, Horgan GW, Dempfle L (2002) Relative Expression Software Tool (REST) for group-wise comparison and statistical analysis of relative expression results in real-time PCR. Nucleic Acids Res **30:** e36

Polle A, Altman A, Jiang XN (2006) Towards genetic engineering for drought tolerance in trees. *In* M Fladung, D Ewald, eds, Tree Transgenesis: Recent Developments. Springer Verlag, Berlin, pp 275–297

Polle A, Schützendübel A (2003) Heavy metal signaling in plants: linking cellular and organismic responses. *In* H Hirt, K Shinozaki, eds, Plant Responses to Abiotic Stresses. Topics in Current Genetics, Vol 4. Springer, Berlin, pp 167–215

Pozo MJ, Azcon-Aguilar C (2007) Unravelling mycorrhiza-induced resistance. Curr Opin Plant Biol **10:** 393–398

Reddy SM, Hitchin S, Melayah D, Pandey AK, Raffier C, Henderson J, Marmeisse R, Gay G (2006) The auxin-inducible GH3 homologue Pp-GH3.16 is down regulated in *Pinus pinaster* root systems on ectomycorrhizal symbiosis establishment. New Phytol **170:** 391–400

Reich M, Göbel C, Kohler A, Buée M, Martin F, Feussner I, Polle A (2009) Fatty acid metabolism in the ectomycorrhizal fungus *Laccaria bicolor*. New Phytol **182:** 950–964

Riedel T, Groten K, Baldwin IT (2008) Symbiosis between *Nicotiana attenuata* and *Glomus intraradices*: ethylene plays a role, jasmonic acid does not. Plant Cell Environ **31:** 1203–1213

Sawada H, Shim IS, Usui K (2006) Induction of benzoic acid 2-hydroxylase and salicylic acid biosynthesis: modulation by salt stress in rice seedlings. Plant Sci **171:** 263–270

Schützendübel A, Polle A (2002) Plant responses to abiotic stresses: heavy metal-induced oxidative stress and protection by mycorrhization. J Exp Bot **53:** 1351–1365

Selle A, Willmann M, Grunze N, Geßler A, Weiß M, Nehls U (2005) The high-affinity poplar ammonium importer *PttAMT1.2* and its role in ectomycorrhizal symbiosis. New Phytol **168:** 697–706

Shah J (2003) The salicylic acid loop in plant defense. Curr Opin Plant Biol **6:** 365–371

Shi L, Guttenberger M, Kottke I, Hampp R (2002) The effect of drought on mycorrhizas of beech (*Fagus sylvatica* L.): changes in community structure, and the content of carbohydrates and nitrogen storage bodies of the fungi. Mycorrhiza **12:** 303–311

Smith SE, Read DJ (2008) Mycorrhizal Symbiosis. Academic Press, New York

Taji T, Ohsumi C, Iuchi S, Seki M, Kasuga M, Kobayashi M, Yamaguchi-Shinozaki K, Shinozaki K (2002) Important roles of drought- and cold-inducible genes for galactinol synthase in stress tolerance in *Arabidopsis thaliana*. Plant J **29:** 417–426

Taji T, Seki M, Satou M, Sakurai T, Kobayashi M, Ishiyama K, Narusaka Y, Narusaka M, Zhu J-K, Shinozaki K (2004) Comparative genomics in salt tolerance between Arabidopsis and Arabidopsis-related halophyte salt cress using Arabidopsis microarray. Plant Physiol **135:** 1697–1709

Teichmann T, Bolu-Arianto WH, Olbrich A, Langenfeld-Heyser R, Göbel C, Grzeganek P, Feussner I, Hänsch R, Polle A (2008) GH3:GUS depicts cell-specific developmental patterns and stress-induced changes in wood anatomy in the poplar stem. Tree Physiol **28:** 1305–1315

Thimm O, Blaesing O, Gibon Y, Nagel A, Meyer S, Krüger P, Selbig J, Müller LA, Rhee SY, Stitt M (2004) MAPMAN: a user-driven tool to

display genomics data sets onto diagrams of metabolic pathways and other biological processes. Plant J **37:** 914–939

Tognolli M, Penel C, Greppin H, Simon P (2002) Analysis and expression of the class III peroxidase large gene family in *Arabidopsis thaliana*. Gene **288:** 129–138

Ton J, Mauch-Mani B (2004) β-Amino-butyric acid-induced resistance against necrotrophic pathogens is based on ABA-dependent priming for callose. Plant J **38:** 119–130

Travaglia C, Cohen AC, Reinoso H, Castillo C, Bottini R (2007) Exogenous abscisic acid increases carbohydrate accumulation and redistribution to the grains in wheat grown under field conditions of soil water restriction. J Plant Growth Regul **26:** 285–289

Tusher VG, Tibshirani R, Chu G (2001) Significance analysis of microarrays applied to the ionizing radiation response. Proc Natl Acad Sci USA **98:** 5116–5121

Usadel B, Nagel A, Thimm O, Redestig H, Blaesing OE, Palacios-Rojas N, Selbig J, Hannemann J, Piques MC, Steinhauser D, et al (2005) Extension of the visualization tool MapMan to allow statistical analysis of arrays, display of corresponding genes, and comparison with known responses. Plant Physiol **138:** 1195–1204

Valdes M, Asbjornsen H, Gomez-Cardenas M, Juarez M, Vogt KA (2006) Drought effects on fine-root and ectomycorrhizal-root biomass in managed *Pinus oaxacana* Mirov stands in Oaxaca, Mexico. Mycorrhiza **16:** 117–124

Vlot AC, Klessig DF, Park SW (2008) Systemic acquired resistance: the elusive signal(s). Curr Opin Plant Biol **11:** 436–442

Wallander H, Nylund JE, Sundberg B (1992) Ectomycorrhiza and nitrogen effects on root IAA: results contrary to current theory. Mycorrhiza **1:** 91–92

Waller F, Achatz B, Baltruschat H, Fodor J, Becker K, Fischer M, Heier T, Huckelhoven R, Neumann C, von Wettstein D, et al (2005) The endophytic fungus *Piriformospora indica* reprograms barley to salt-stress tolerance, disease resistance, and higher yield. Proc Natl Acad Sci USA **102:** 13386–13391

Wang C, Ying S, Huang HJ, Li K, Wu P, Shou HX (2009) Involvement of OsSPX1 in phosphate homeostasis in rice. Plant J **57:** 895–904

Wang D, Amornsiripanitch N, Dong X (2006) A genomic approach to identify regulatory nodes in the transcriptional network of systemic acquired resistance in plants. PLoS Pathog **2:** e123

Wang Y, Ribot C, Rezzonico E, Poirier Y (2004) Structure and expression profile of the *Arabidopsis* PHO1 gene family indicates a broad role in inorganic phosphate homeostasis. Plant Physiol **135:** 400–411

Winter H, Lohaus G, Heldt HW (1992) Phloem transport of amino acids in relation to their cytosolic levels in barley leaves. Plant Physiol **99:** 996–1004

Woodward AW, Ratzel SE, Woodward EE, Shamoo Y, Bartel B (2007) Mutation of E1-CONJUGATING ENZYME-RELATED1 decreases RELATED TO UBIQUITIN conjugation and alters auxin response and development. Plant Physiol **144:** 976–987

Wright DP, Johansson T, Le Quere A, Soderstrom B, Tunlid A (2005) Spatial patterns of gene expression in the extramatrical mycelium and mycorrhizal root tips formed by the ectomycorrhizal fungus *Paxillus involutus* in association with birch (*Betula pendula*) seedlings in soil microcosms. New Phytol **167:** 579–596

Xiong LM, Schumaker KS, Zhu JK (2002) Cell signaling during cold, drought, and salt stress. Plant Cell (Suppl) **14:** S165–S183

Yamaguchi-Shinozaki K, Koizumi M, Urao S, Shinozaki K (1992) Molecular cloning and characterization of 9 cDNAs for genes that are responsive to desiccation in *Arabidopsis thaliana*: sequence analysis of one cDNA clone that encodes a putative transmembrane channel protein. Plant Cell Physiol **33:** 217–224

Yamaguchi-Shinozaki K, Shinozaki K (2006) Transcriptional regulatory networks in cellular responses and tolerance to dehydration and cold stresses. Annu Rev Plant Biol **57:** 781–803

Yang JY, Iwasaki M, Machida C, Machida Y, Zhou X, Chua N (2008) BetaC1, the pathogenicity factor of TYLCCNV, interacts with AS1 to alter leaf development and suppress selective jasmonic acid responses. Genes Dev **22:** 2564–2577

Zhang S, Yang X, Sun M, Sun F, Deng S, Dong H (2009) Riboflavin-induced priming for pathogen defense in *Arabidopsis thaliana*. J Integr Plant Biol **51:** 167–174